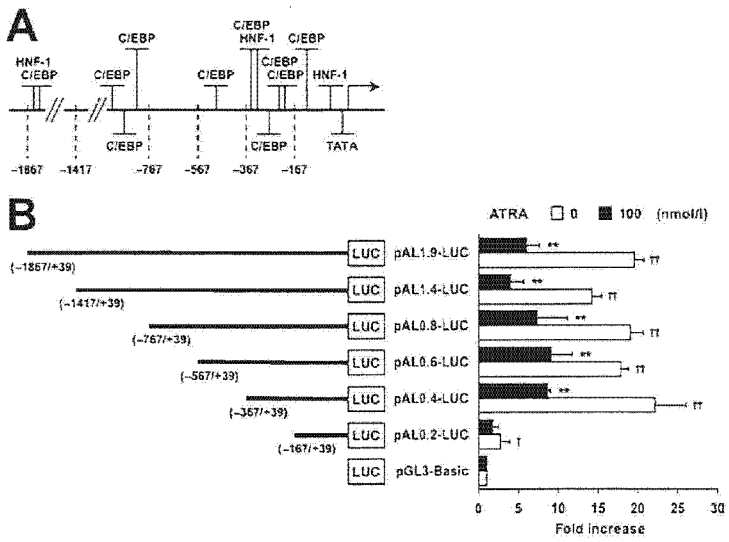

Figure 2 Identification of the 5′ end flanking region of the albumin gene responsible for its transcriptional down-regulation by ATRA

(**A**) Schematic diagram of the potential binding sites for liver-enriched transcription factors in the 5′ end flanking region of the albumin gene analysed with a computer search program, TFSEARCH. (**B**) Deletion constructs of the upstream regulatory region of the albumin gene linked to the firefly luciferase reporter gene (LUC) are shown. FLC-4 cells were co-transfected with a *Renilla* luciferase internal control reporter (pRL-CMV) and a firefly luciferase reporter. Then, cells were stimulated with (black columns) or without (white columns) 100 nmol/l ATRA for 48 h. The relative luciferase activity was obtained by normalizing the firefly luciferase activity to the *Renilla* luciferase activity. The value of the empty vector (pGL3-Basic) was set to 1. $^{**}P < 0.01$ compared with transfected cells not exposed to ATRA. $\dagger P < 0.05$; $\dagger\dagger P < 0.01$ compared with cells transfected with empty vector.

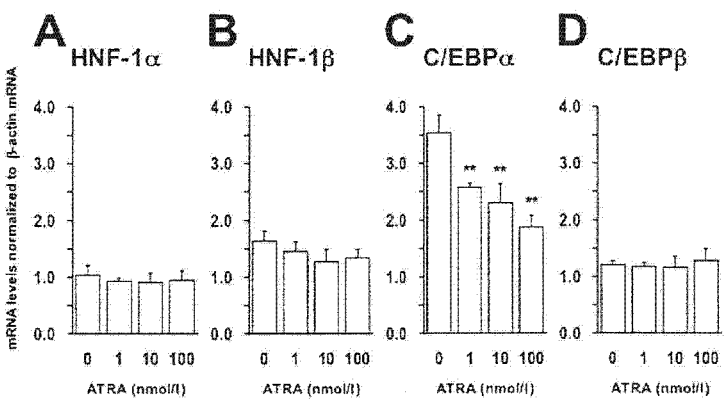

Figure 3 mRNA levels of liver-enriched transcription factors in FLC-4 cells treated with ATRA

The cells were harvested after treatment with ATRA for 24 h, and the mRNA levels of HNF-1α (**A**), HNF-1β (**B**), C/EBPα (**C**) and C/EBPβ (**D**) were measured by quantitative RT-PCR analysis. The mRNA level of each of these liver-enriched transcription factors was normalized to β-actin mRNA level. $^{**}P < 0.01$ compared with untreated control cells.

transcriptional repression by ATRA and that this region is important for a high level of expression of the human albumin gene.

Effect of ATRA on the expression of transcription factors that possibly bind to the albumin promoter

Several potential *cis*-elements within nt -367 to -167 were identified by sequence analysis using TFSEARCH. This region contained binding sites for liver-specific transcription factors, C/EBPs and HNF-1s, as indicated in Figure 2(A). We next examined whether ATRA regulates expression of these transcription factors at the transcriptional level using quantitative real-time RT-PCR (Figure 3). As shown in Figure 3(C), the mRNA level of C/EBPα, which had the most abundant expression of the four transcription factors tested, was significantly decreased by ATRA treatment in a dose-dependent manner; C/EBPα mRNA expression in FLC-4 cells was suppressed by 47 % in the presence of 100 nmol/l ATRA. By contrast, ATRA exhibited no effect or only a marginal effect on the mRNA levels of HNF-1α, HNF-1β and C/EBPβ (Figure 3A, B and D). Since C/EBPα is known to be a positive regulator of human albumin expression [32,33], it may be possible that down-regulation of C/EBPα expression is one of the mechanisms involved in the inhibitory effect of ATRA on human albumin synthesis.

In vivo recruitment of C/EBPs to the human albumin promoter

To investigate whether the inhibitory effect of ATRA on albumin expression is associated with the recruitment of C/EBPs to

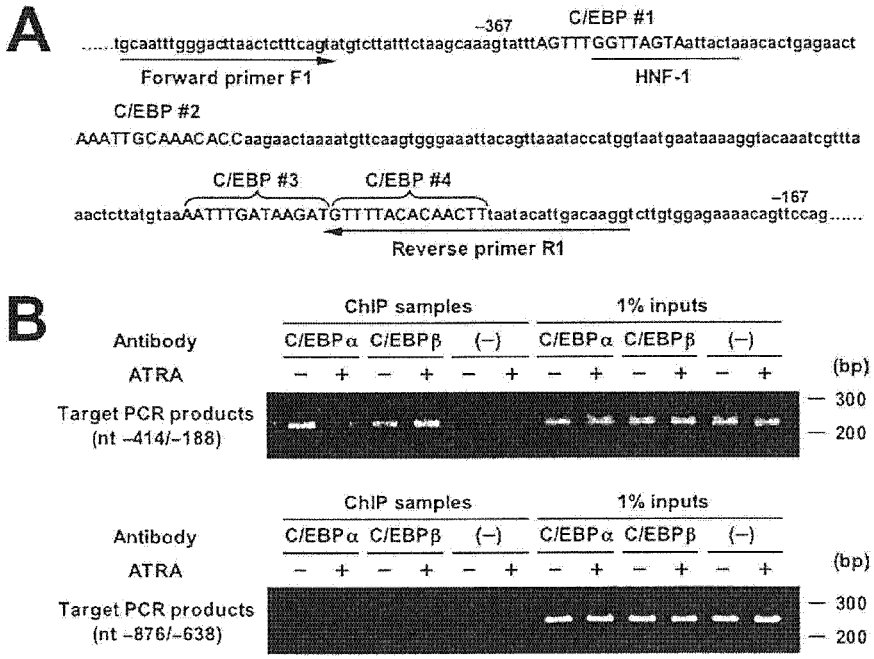

Figure 4 Effects of ATRA on *in vivo* recruitment of C/EBPs to the human albumin promoter

(**A**) The sequence of the upstream regulatory region (between nt −414 and −188) of human albumin was amplified using a PCR primer pair (F1 and R1), indicated by the arrows. The potential binding sites for C/EBP and HNF-1 in this region are in capital letters and underlined respectively. (**B**) FLC-4 cells were incubated with or without ATRA (100 nmol/l) for 48 h before the ChIP assay. DNA fragments were amplified with the primers F1 and R1 (upper panel) or F2 and R2 (lower panel). The input represents PCR products from chromatin pellets before immunoprecipitation.

the albumin promoter *in vivo*, we performed ChIP assays of cells treated with or without ATRA (Figure 4). After immunoprecipitation with antibodies against C/EBPα and C/EBPβ, the −414 to −188 nt fragment within the albumin promoter, which contains four potential binding sites for C/EBPs (C/EBP #1–#4 in Figure 4A), was amplified by PCR. The results revealed that under basal conditions both endogenous C/EBPα and C/EBPβ were recruited to the albumin promoter. It is of interest that the *in vivo* binding of C/EBPα to the fragment was markedly decreased upon incubation with ATRA. By contrast, ATRA treatment seemed to marginally increase the recruitment of C/EBPβ to the promoter fragment (Figure 4B). We verified that no DNA fragment was detected in the precipitated chromatin when the region between nt −876 and −638 of the albumin gene, which does not contain binding sites for C/EBP, was amplified by PCR.

These findings suggest that ATRA has the ability to affect the C/EBP occupancy of the albumin promoter *in vivo*. It is possible that impaired C/EBPα binding caused by ATRA leads to down-regulation of albumin gene expression.

ATRA induces expression of C/EBPβ-LIP, and its DNA-binding activity

It has been reported that the gene for C/EBP is transcribed into a single mRNA that encodes several N-terminally truncated protein isoforms, possibly via the process of alternative translation initiation at downstream AUG codons [34,35]. C/EBPα mRNA is translated into two major proteins of 42 and 30 kDa (p42- and p30-C/EBPα) [34,36], whereas C/EBPβ mRNA mainly produces three isoforms referred to as C/EBPβ-FL, LAP (liver-enriched transcriptional activator protein) and LIP, which are 46, 42, and 20 kDa respectively [34,37,38]. All of the C/EBP isoforms have DNA-binding and dimerization domains. However, p30-C/EBPα and LIP are translated from the third in-frame AUG start codon [34,36] and lack most of the transactivation domain [34,37,39]. Although p42-C/EBPα, C/EBPβ-FL and LAP transactivate their target genes' expression, p30-C/EBPα and LIP are unable to activate gene transcription and are able to function as dominant-negative factors by antagonizing and by competing with other C/EBP transactivators [34,37]. It has been considered that the ratio of C/EBP transactivators to C/EBP dominant-negative factors is important in controlling each activity of C/EBPα and C/EBPβ [34,36,37].

We determined the effect of ATRA on the expression of C/EBP isoforms by Western blotting (Figure 5A). An increased level of LIP was observed as early as 8 h after ATRA treatment and it was also detected after 48 h of treatment. By contrast, C/EBPβ-FL and LAP isoforms showed little change in their expression after the 48 h time point of ATRA treatment. The expression level of C/EBPα showed no change in the presence of ATRA after 8 or 16 h. Although a decrease in C/EBPα expression was found after 48 h of ATRA treatment, it is not likely that this reduction is the cause of down-regulation of albumin expression, since a decreased level of albumin mRNA was observed as early as 24 h after ATRA treatment (Figure 1B). It appears that the ratio of LIP to C/EBPβ-FL and LAP was elevated in a dose-dependent manner after 16 h of ATRA treatment, while the ratio of p42-C/EBPα to p30-C/EBPα showed no difference with or without ATRA treatment until 48 h after the addition of ATRA. These results demonstrate that ATRA has the ability to differentially modulate the level of C/EBP isoforms with an increase in LIP and a decrease in C/EBPα; the expression of LIP is induced immediately in response to ATRA treatment.

We next examined the effect of ATRA on the DNA-binding activity of LIP, by EMSA (Figure 5B). The nucleotide sequence of C/EBP-binding site #3, which is present in the region from

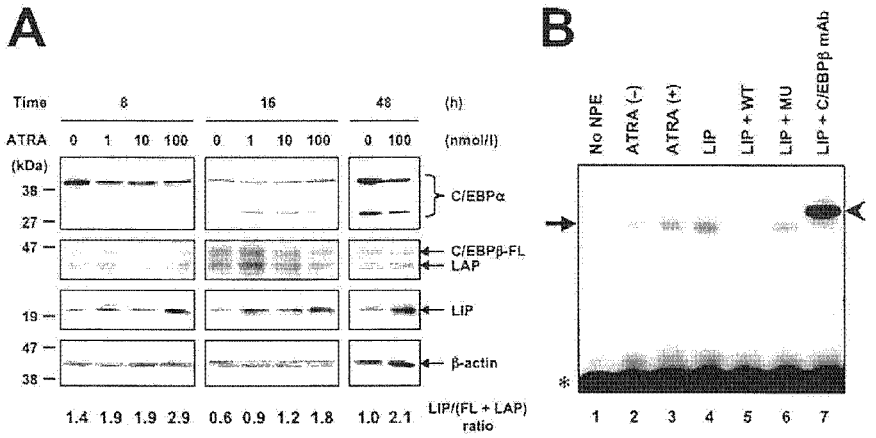

Figure 5 Effect of ATRA on protein expression of C/EBPs, and DNA-binding activity of C/EBPβ-LIP

(**A**) FLC-4 cells were incubated with ATRA (100 nmol/l) for 8, 16 and 48 h. After harvesting, total cellular proteins were resolved by SDS/PAGE, and the presence of C/EBPα and C/EBPβ was analysed by Western blotting. The ratio of C/EBPβ-LIP to C/EBPβ-FL and -LAP [LIP/(FL + LAP)] was measured by densitometric analysis. (**B**) Nuclear proteins were extracted from FLC-4 cells treated with or without 100 nmol/l ATRA for 48 h, or cells that transiently expressed the LIP protein, and were analysed by EMSA as described in the Experimental section. Lane 1, no nuclear protein extracts (NPE); lane 2, FLC-4 cells incubated without ATRA; lane 3, FLC-4 cells incubated with ATRA; lane 4, FLC-4 cells transiently expressing the LIP protein; lane 5, addition of a 50-fold molar excess of unlabelled wild-type (WT) oligonucleotides to the mixture in lane 4; lane 6, addition of a 50-fold molar excess of unlabelled mutant (MU) oligonucleotides to the mixture in lane 4; lane 7, addition of an anti-C/EBPβ monoclonal antibody (mAb) to the mixture in lane 4. The arrow, arrowhead and asterisk indicate a DNA–LIP complex, a DNA–LIP-antibody complex (supershifted band) and a free probe respectively.

nt −367 to −167 of the albumin gene, as shown in Figure 4(A), was used as a DNA probe. A shifted band, which was observed in FLC-4 cells that transiently express LIP protein (Figure 5, lane 4), was removed by the addition of an excess of unlabelled homologous probe (lane 5), but not by the addition of a mutated sequence (lane 6). This band was supershifted by the addition of the C/EBPβ antibody (lane 7). The results indicate that LIP binds to its binding motif within the albumin promoter.

In the presence of ATRA (Figure 5, lane 3), a shifted band that corresponded to endogenous LIP-bound DNA was observed, which was more intense than in the absence of ATRA (lane 2). We also confirmed that endogenous LIP bound to the other three binding sites for C/EBP (#1, #2 and #4) (results not shown). Thus the combined data demonstrate that ATRA induces not only the expression of LIP but also its DNA-binding activity.

C/EBPβ-LIP down-regulates the gene expression and synthesis of albumin by blocking the transcriptional activity of C/EBPα and C/EBPβ-FL

Our data suggest that early induction of LIP expression and an increase in the DNA-binding activity of LIP caused by ATRA triggers the down-regulation of albumin gene expression. To directly evaluate the role of LIP in albumin expression, we determined the effect of C/EBPs on albumin expression using transient transfection experiments (Figure 6). As shown in Figure 6(A), overexpression of C/EBPα and C/EBPβ-FL caused a more than 20.7- or 8-fold increase respectively, in promoter activity in a dose-dependent manner compared with transfection with an empty vector. By contrast, co-expression with LIP resulted in a marked and dose-dependent reduction of the increased activity (Figure 6B). Expression of LIP alone also decreased the level of promoter activity (Figure 6B), presumably because LIP inhibited positive functions of endogenous C/EBP transactivators expressed in FLC-4 cells. We investigated the effect of C/EBP expression on the secretion of endogenous albumin (Figure 6C). Consistent with albumin promoter activity, overexpression of C/EBPα and C/EBPβ-FL significantly increased the level of albumin in the culture mediun by 2- and 1.7-fold respectively, compared with transfection with an empty vector. Overexpression of LIP significantly and dose-dependently decreased both the basal level of albumin secretion and the level of albumin elevated by expression of C/EBPα and C/EBPβ-FL. Thus these results strongly suggest that LIP plays a role in repressing albumin gene expression by blocking the ability of C/EBP transactivators to activate the albumin promoter, leading to down-regulation of albumin synthesis.

DISCUSSION

In the present study, we have demonstrated the down-regulation of secretion and gene expression of albumin mediated by ATRA. This finding is in line with previous reports that ATRA negatively regulates albumin synthesis in rat hepatocytes [20] and human hepatoma cell lines [12,13]. We addressed its molecular mechanisms and found: (i) that the 5′ end flanking region of the albumin gene, nt −367 to −167, in which four binding sites for C/EBPs are conserved, is responsible for its transcriptional repression by ATRA, and (ii) that upon ATRA treatment, C/EBPβ-LIP is differentially induced among C/EBPβ isoforms and the expression of C/EBPα is subsequently decreased. The present study reveals that C/EBP proteins play a key role in the transcriptional regulation of the human albumin gene by ATRA.

C/EBPα and C/EBPβ, which are composed of DNA-binding and dimerization domains at their C-termini, and transactivation domains at their N-terminal regions, are expressed in the liver at high levels and are involved in the regulation of cell growth, cell differentiation, metabolism and inflammation [40–42]. A single mRNA species for C/EBPβ directs production of three major isoforms in liver tissues: C/EBPβ-FL, LAP and a low-molecular-mass isoform, LIP [34,37,38]. These three proteins contain the DNA-binding and dimerization domains. C/EBPβ-FL and LAP contain a transactivation domain and function as transcriptional activators, whereas LIP lacks the N-terminal transactivation domain and can attenuate the transcriptional stimulation by

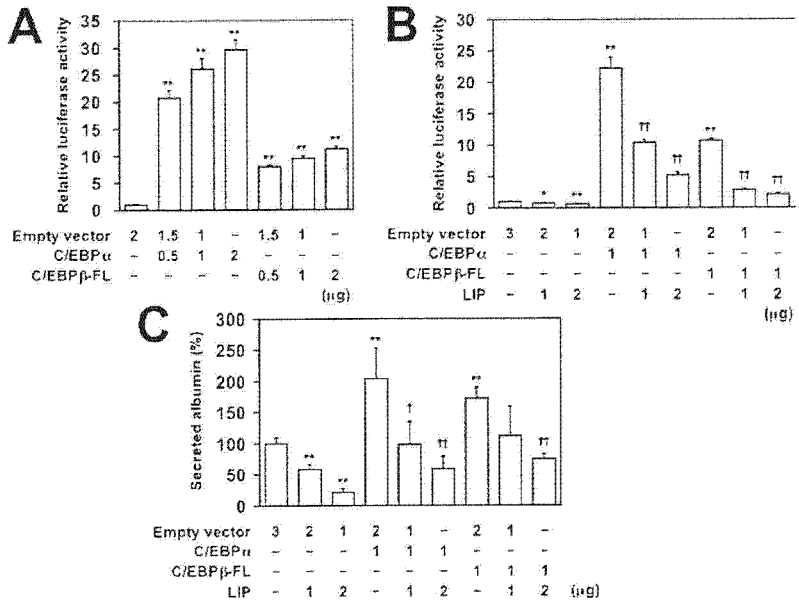

Figure 6 C/EBPβ-LIP down-regulates the promoter activity and synthesis of albumin by blocking C/EBP transcriptional activity

(**A**) and (**B**) FLC-4 cells were transfected with pAL1.9-LUC and pRL-CMV in the presence or absence of C/EBP expression vectors. After incubation for 48 h, the cells were harvested and assayed for luciferase activity. The relative luciferase activity was obtained by normalizing the pAL1.9-LUC activity to the pRL-CMV activity, and the value of the empty vector (pCAGGS) was set to 1. $*P < 0.05$; $**P < 0.01$ compared with cells transfected with empty vector. $††P < 0.01$ compared with cells expressing C/EBPα or C/EBPβ-FL alone. (**C**) FLC-4 cells were transfected with C/EBP expression vectors and/or an empty vector. After 72 h, the medium was harvested, and the amount of secreted albumin was quantified by ELISA. The value of the empty vector was set to 100%. $**P < 0.01$ compared with transfection with empty vector. $†P < 0.05$; $††P < 0.01$ compared with cultures that express C/EBPα or C/EBPβ-FL alone.

C/EBPβ-FL, LAP and C/EBPα in substoichiometric amounts [37]. It has been shown that LIP is involved in the down-regulation of human *CYP3A4* induced by interleukin-6 [43] and in the repression of C/EBPα mRNA during the acute phase of the immune response [44]. In the present study, we have demonstrated that the overexpression of LIP leads to inhibition of the positive regulation of albumin promoter activity that is mediated by C/EBPα and C/EBPβ-FL (Figure 6B). This is the first study to show the involvement of LIP in the regulation of human albumin gene expression.

Our albumin promoter assay using the 5′end-deletion constructs demonstrated that the region spanning nt −367 to −167 within the albumin gene is a prerequisite for ATRA-dependent transcriptional down-regulation (Figure 2B). The ChIP assay showed that during ATRA treatment the *in vivo* binding of C/EBPα to the region clearly decreased, whereas the binding of C/EBPβ slightly increased (Figure 4B). The anti-C/EBPβ antibody used in the present study is capable of recognizing all of the C/EBPβ isoforms, since no anti-C/EBPβ antibodies that recognize the N-termini of C/EBPβ are available to distinguish these isoforms. However, an EMSA demonstrated that ATRA increased the binding activity of LIP to its response element in this region (Figure 5B). Thus we suggest that the increase in DNA-binding of C/EBPβ, as shown in the ChIP assay, is caused by ATRA-induced LIP expression. It has been reported that LIP has a greater binding capacity for the C/EBP-binding element compared with C/EBP transactivators i.e. LIP binds to the element 4-fold more efficiently than does LAP [37]. Therefore it is probable that C/EBP transactivators predominantly bind to their response elements within the albumin promoter in the ATRA-untreated cells, while an increased level of LIP possibly displaces these transactivators at the C/EBP-binding sites to occuy them in ATRA-treated cells.

As indicated in Figure 5(A), preferential induction of LIP expression by ATRA was observed even in the culture after

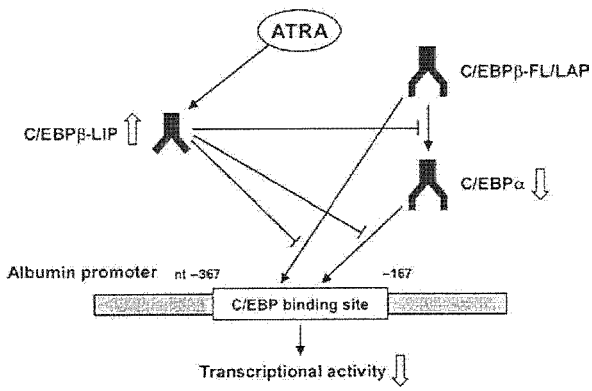

Figure 7 Proposed mechanism by which ATRA down-regulates albumin gene transcription in FLC-4 cells

An ATRA signal increases the expression of C/EBPβ-LIP in FLC-4 cells. This truncated C/EBP protein directly and indirectly down-regulates the expression of the albumin gene by competing with C/EBP transactivators and inhibiting C/EBPα expression.

8 h of ATRA treatment. By contrast, a decrease in C/EBPα gene expression was not detected at such an early stage (results not shown), but was first observed 24 h after the addition of ATRA (Figure 3C). Furthermore, the expression level of C/EBPα protein was little changed when the mRNA expression level of albumin was decreased by ATRA treatment (Figure 5A). Based on the results of the present study, we propose a model for the molecular mechanism by which ATRA down-regulates the expression of human albumin in liver-derived cells (Figure 7). ATRA triggers the differential induction of C/EBPβ-LIP, a dominant-negative regulator of C/EBP activators. A C/EBP-binding consensus sequence has been identified in the C/EBPα

promoter, and it has been shown that C/EBPβ-FL and LIP respectively, function as positive and negative regulators of C/EBPα gene expression [44]. Thus it is probable that LIP preferentially binds to the C/EBP-binding elements not only on the albumin promoter but also on that of C/EBPα at the expense of C/EBPβ-FL, LAP and C/EBPα. However, LIP lacks the transactivation domain and is unable to activate transcription. LIP expression induced by ATRA possibly down-regulates the gene expression of albumin and C/EBPα, by competing for DNA-binding sites as a LIP homodimer and/or by antagonizing the transcriptional activity of C/EBP transactivators via heterodimer formation with C/EBP-FL or LAP [37]. Hence, an increase in the ratio of LIP to C/EBP transactivators is critical for down-regulation of the expression of albumin and C/EBPα genes that is mediated by ATRA. This conclusion is supported by transient transfection experiments which indicated that the activity of the albumin promoter is stimulated by transfection with C/EBPβ-FL or C/EBPα expression constructs (Figure 6A), whereas its activity is decreased by co-transfection with a LIP construct (Figure 6B). Decreased expression of C/EBPα may also contribute to the transcriptional repression of the albumin gene, since C/EBPα is known to be one of the positive regulators of albumin expression [32,33].

A key question is: how does ATRA differentially induce C/EBPβ-LIP but not C/EBPβ-FL expression? A previous study [45], which describes the effect of ATRA on the alternate production of C/EBPβ isoforms, has not demonstrated its molecular mechanism. A number of recent observations have shown that the production of C/EBPβ isoforms is regulated by epidermal growth factor [38], lipopolysacharide [44,46] and partial hepatectomy [44,47], presumably through leaky ribosomal scanning [34,37]. It has been proposed that a portion of ribosomes ignore the first two AUG codons of the C/EBPβ mRNA and initiate translation of LIP from the third in-frame AUG start codon. The translation of LIP can be controlled by specific cytoplasmic proteins that interact with the 5′ end region of C/EBPβ mRNA, such as CUG-BP1 (CUG triplet-repeat binding protein 1) [44,47]. Phosphorylation of CUG-BP1 is critical for its RNA binding and the consequent increase in LIP expression [38]. Therefore we tested whether ATRA treatment leads to increased phosphorylation of CUG-BP1 in FLC-4 cells. Western blotting and immunoprecipitation of CUG-BP1 metabolically labelled with ^{32}P, however, indicated that the expression level and phosphorylation status of CUG-BP1 were not different in cells with or without ATRA treatment (results not shown). It can be speculated that other RNA-binding proteins are involved in the mechanism by which ATRA increases the translation of LIP because, in addition to CUG-BP1, calreticulin [48] and eIFs (eukaryotic translation initiation factors), such as eIF-2 and eIF-4E [35], have been shown to control translation of C/EBPβ. Another possible mechanism for the alternate production of C/EBPβ isoforms is the proteolytic cleavage of C/EBPβ-FL [49]. However, this is less likely to explain the mechanism for the differential induction of LIP isoforms caused by ATRA, because it has been shown that the cleavage of C/EBPβ-FL to generate LIP is induced by C/EBPα [49], but that the ATRA treatment led to no change or only a small decrease in the expression of C/EBPα (Figure 5A).

A previous study [13] has shown that the expression of HNF-1, which is a potent transcription factor for the albumin gene [50], was decreased in human hepatoma cells in which albumin gene expression was down-regulated by ATRA, although an upstream regulatory region of the albumin gene involved in the regulation was not identified. In our experimental setting, mRNA expression of HNF-1 was not affected by ATRA treatment (Figures 3A and 3B). The data in the present study suggest a model in which the preferential increase in LIP expression mediated by ATRA results in the antagonization of C/EBP transactivators by interaction with their binding sites on the nt -367 to -167 region of the albumin promoter. We propose a novel pathway for the modulation of gene expression by ATRA, in which C/EBPβ-LIP plays a crucial role. This mechanism may be found in other systems for physiological processes, such as cell proliferation and differentiation, and the elucidation of its molecular mechanism will make a great contribution to our understanding of gene regulation mediated by retinoic acids.

We thank G. J. Darlington for providing the plasmids, and A. Catharine Ross (Department of Nutritional Sciences, The Pennsylvania State University) and our colleagues for helpful discussions. We also thank M. Matsuda, M. Ikeda, S. Yoshizaki and T. Shimoji for their technical assistance. This work was supported by grants-in-aid from the Ministry of Health, Labor and Welfare, by the Program for Promotion of Fundamental Studies in Health Sciences of the Organization for Drug ADR Relief, R&D Promotion and Product Review of Japan (ID:01-3), and by Research on Health Sciences focusing on Drug Innovation from the Japan Health Sciences Foundation, Japan. T.M. is the recipient of a Research Resident Fellowship from the Foundation for Promotion of Cancer Research in Japan.

REFERENCES

1 West, J. B. (1990) Blood and the plasma proteins: functions and composition of blood. In Physiological Basis of Medical Practice. In (West, J. B., ed.), pp. 332–338, Williams & Wilkins, Baltimore
2 Rothschild, M. A., Oratz, M. and Schreiber, S. S. (1988) Serum albumin. Hepatology **8**, 385–401
3 Moshage, H. J., Janssen, J. A., Franssen, J. H., Hafkenscheid, J. C. and Yap, S. H. (1987) Study of the molecular mechanism of decreased liver synthesis of albumin in inflammation. J. Clin. Invest. **79**, 1635–1641
4 Mariani, G., Strober, W., Keiser, H. and Waldmann, T. A. (1976) Pathophysiology of hypoalbuminemia associated with carcinoid tumor. Cancer **38**, 854–860
5 Chlebowski, R. T., Grosvenor, M. B., Bernhard, N. H., Morales, L. S. and Bulcavage, L. M. (1989) Nutritional status, gastrointestinal dysfunction, and survival in patients with AIDS. Am. J. Gastroenterol. **84**, 1288–1293
6 Phillips, A., Shaper, A. G. and Whincup, P. H. (1989) Association between serum albumin and mortality from cardiovascular disease, cancer, and other causes. Lancet **2**, 1434–1436
7 Gorski, K., Carneiro, M. and Schibler, U. (1986) Tissue-specific *in vitro* transcription from the mouse albumin promoter. Cell **47**, 767–776
8 Maire, P., Wuarin, J. and Schibler, U. (1989) The role of *cis*-acting promoter elements in tissue-specific albumin gene expression. Science **244**, 343–346
9 Perlmutter, D. H., Dinarello, C. A., Punsal, P. I. and Colten, H. R. (1986) Cachectin/tumor necrosis factor regulates hepatic acute-phase gene expression. J. Clin. Invest. **78**, 1349–1354
10 Andus, T., Geiger, T., Hirano, T., Kishimoto, T. and Heinrich, P. C. (1988) Action of recombinant human interleukin 6, interleukin 1β and tumor necrosis factor α on the mRNA induction of acute-phase proteins. Eur. J. Immunol. **18**, 739–746
11 Morrone, G., Cortese, R. and Sorrentino, V. (1989) Post-transcriptional control of negative acute phase genes by transforming growth factor β. EMBO J. **8**, 3767–3771
12 Hsu, S. L., Lin, Y. F. and Chou, C. K. (1992) Transcriptional regulation of transferrin and albumin genes by retinoic acid in human hepatoma cell line Hep3B. Biochem. J. **283**, 611–615
13 Yamada, Y., Shidoji, Y., Fukutomi, Y., Ishikawa, T., Kaneko, T., Nakagama, H., Imawari, M., Moriwaki, H. and Muto, Y. (1994) Positive and negative regulations of albumin gene expression by retinoids in human hepatoma cell lines. Mol. Carcinog. **10**, 151–158
14 Molina, A., Oka, T., Muñoz, S. M., Chikamori-Aoyama, M., Kuwahata, M. and Natori, Y. (1997) Vitamin B_6 suppresses growth and expression of albumin gene in a human hepatoma cell line HepG2. Nutr. Cancer **28**, 206–211
15 Tsutsumi, T., Nakao, K., Mitsuoka, S., Hamasaki, K., Tsuruta, S., Shima, M., Nakata, K., Tamaoki, T. and Nagataki, S. (1993) Regulation of albumin and α-fetoprotein gene expression by colloid osmotic pressure in human hepatoma cells. Gastroenterology **104**, 256–262
16 Pietrangelo, A. and Shafritz, D. A. (1994) Homeostatic regulation of hepatocyte nuclear transcription factor 1 expression in cultured hepatoma cells. Proc. Natl. Acad. Sci. U.S.A. **91**, 182–186
17 Marten, N. W., Hsiang, C. H., Yu, L., Stollenwerk, N. S. and Straus, D. S. (1999) Functional activity of hepatocyte nuclear factor-1 is specifically decreased in amino acid-limited hepatoma cells. Biochim. Biophys. Acta **1447**, 160–174

18 Falasca, L., Favale, A., Gualandi, G., Maletta, G. and Conti Devirgiliis, L. (1998) Retinoic acid treatment induces apoptosis or expression of a more differentiated phenotype on different fractions of cultured fetal rat hepatocytes. Hepatology **28**, 727–737
19 Alisi, A., Leoni, S., Piacentani, A. and Conti Devirgiliis, L. (2003) Retinoic acid modulates the cell-cycle in fetal rat hepatocytes and HepG2 cells by regulating cyclin-cdk activities. Liver Int. **23**, 179–186
20 Ikeda, H. and Fujiwara, K. (1993) Retinoic acid inhibits DNA and albumin synthesis stimulated by growth factor in adult rat hepatocytes in primary culture. Biochem. Biophys. Res. Commun. **191**, 675–680
21 Sani, B. P. and Meeks, R. G. (1983) Subacute toxicity of all-*trans*- and 13-*cis*-isomers of *N*-ethyl retinamide, *N*-2-hydroxyethyl retinamide, and *N*-4-hydroxyphenyl retinamide. Toxicol. Appl. Pharmacol. **70**, 228–235
22 Decensi, A., Bruno, S., Costantini, M., Torrisi, R., Curotto, A., Gatteschi, B., Nicolò, G., Polizzi, A., Perloff, M., Malone, W. F. and Bruzzi, P. (1994) Phase IIa study of fenretinide in superficial bladder cancer, using DNA flow cytometry as an intermediate end point. J. Natl. Cancer Inst. **86**, 138–140
23 Kalemkerian, G. P., Slusher, R., Ramalingam, S., Gadgeel, S. and Mabry, M. (1995) Growth inhibition and induction of apoptosis by fenretinide in small-cell lung cancer cell lines. J. Natl. Cancer Inst. **87**, 1674–1680
24 Maurer, B. J., Metelitsa, L. S., Seeger, R. C., Cabot, M. C. and Reynolds, C. P. (1999) Increase of ceramide and induction of mixed apoptosis/necrosis by *N*-(4-hydroxyphenyl)-retinamide in neuroblastoma cell lines. J. Natl. Cancer Inst. **91**, 1138–1146
25 Puduvalli, V. K., Yung, W. K., Hess, K. R., Kuhn, J. G., Groves, M. D., Levin, V. A., Zwiebel, J., Chang, S. M., Cloughesy, T. F., Junck, L. et al. (2004) Phase II study of fenretinide (NSC 374551) in adults with recurrent malignant gliomas: a North American brain tumor consortium study. J. Clin. Oncol. **22**, 4282–4289
26 Nagamori, S., Hasumura, S., Matsuura, T., Aizaki, H. and Kawada, M. (2000) Developments in bioartificial liver research: concepts, performance, and applications. J. Gastroenterol. **35**, 493–503
27 Aizaki, H., Nagamori, S., Matsuda, M., Kawakami, H., Hashimoto, O., Ishiko, H., Kawada, M., Matsuura, T., Hasumura, S., Matsuura, Y. et al. (2003) Production and release of infectious hepatitis C virus from human liver cell cultures in the three-dimensional radial-flow bioreactor. Virology **314**, 16–25
28 Niwa, H., Yamamura, K. and Miyazaki, J. (1991) Efficient selection for high-expression transfectants with a novel eukaryotic vector. Gene **108**, 193–199
29 Iwahori, T., Matsuura, T., Maehashi, H., Sugo, K., Saito, M., Hosokawa, M., Chiba, K., Masaki, T., Aizaki, H., Ohkawa, K. and Suzuki, T. (2003) CYP3A4 inducible model for *in vitro* analysis of human drug metabolism using a bioartificial liver. Hepatology **37**, 665–673
30 Mangelsdorf, D. J. and Evans, R. M. (1995) The RXR heterodimers and orphan receptors. Cell **83**, 841–850
31 Chambon, P. (1996) A decade of molecular biology of retinoic acid receptors. FASEB J. **10**, 940–954
32 Friedman, A. D., Landschulz, W. H. and McKnight, S. L. (1989) CCAAT/enhancer binding protein activates the promoter of the serum albumin gene in cultured hepatoma cells. Genes Dev. **3**, 1314–1322
33 Trautwein, C., Rakemann, T., Pietrangelo, A., Plümpe, J., Montosi, G. and Manns, M. P. (1996) C/EBP-β/LAP controls down-regulation of albumin gene transcription during liver regeneration. J. Biol. Chem. **271**, 22262–22270
34 Ossipow, V., Descombes, P. and Schibler, U. (1993) CCAAT/enhancer-binding protein mRNA is translated into multiple proteins with different transcription activation potentials. Proc. Natl. Acad. Sci. U.S.A. **90**, 8219–8223
35 Calkhoven, C. F., Müller, C. and Leutz, A. (2000) Translational control of C/EBPα and C/EBPβ isoform expression. Genes Dev. **14**, 1920–1932
36 Lin, F. T., MacDougald, O. A., Diehl, A. M. and Lane, M. D. (1993) A 30-kDa alternative translation product of the CCAAT/enhancer binding protein α message: transcriptional activator lacking antimitotic activity. Proc. Natl. Acad. Sci. U.S.A. **90**, 9606–9610
37 Descombes, P. and Schibler, U. (1991) A liver-enriched transcriptional activator protein, LAP, and a transcriptional inhibitory protein, LIP, are translated from the same mRNA. Cell **67**, 569–579
38 Baldwin, B. R., Timchenko, N. A. and Zahnow, C. A. (2004) Epidermal growth factor receptor stimulation activates the RNA binding protein CUG-BP1 and increases expression of C/EBPβ-LIP in mammary epithelial cells. Mol. Cell. Biol. **24**, 3682–3691
39 Calkhoven, C. F., Bouwman, P. R., Snippe, L. and Ab, G. (1994) Translation start site multiplicity of the CCAAT/enhancer binding protein α mRNA is dictated by a small 5′ open reading frame. Nucleic Acids Res. **22**, 5540–5547
40 Wang, N. D., Finegold, M. J., Bradley, A., Ou, C. N., Abdelsayed, S. V., Wilde, M. D., Taylor, L. R., Wilson, D. R. and Darlington, G. J. (1995) Impaired energy homeostasis in C/EBPα knockout mice. Science **269**, 1108–1112
41 Poli, V. (1998) The role of C/EBP isoforms in the control of inflammatory and native immunity functions. J. Biol. Chem. **273**, 29279–29282
42 Wang, H., Iakova, P., Wilde, M., Welm, A., Goode, T., Roesler, W. J. and Timchenko, N. A. (2001) C/EBPα arrests cell proliferation through direct inhibition of Cdk2 and Cdk4. Mol. Cell **8**, 817–828
43 Jover, R., Borl, R., Gómez-Lechón, M. J. and Castell, J. V. (2002) Down-regulation of human CYP3A4 by the inflammatory signal interleukin 6: molecular mechanism and transcription factors involved. FASEB J. **16**, 1799–1801
44 Welm, A. L., Mackey, S. L., Timchenko, L. T., Darlington, G. J. and Timchenko, N. A. (2000) Translational induction of liver-enriched transcriptional inhibitory protein during acute phase response leads to repression of CCAAT/enhancer binding protein α mRNA. J. Biol. Chem. **275**, 27406–27413
45 Hsu, W. and Chen-Kiang, S. (1993) Convergent regulation of NF-IL6 and Oct-1 synthesis by interleukin-6 and retinoic acid signaling in embryonal carcinoma cells. Mol. Cell. Biol. **13**, 2515–2523
46 Hsieh, C. C., Xiong, W., Xie, Q., Rabek, J. P., Scott, S. G., An, M. R., Reisner, P. D., Kuninger, D. T. and Papaconstantinou, J. (1998) Effects of age on the posttranscriptional regulation of CCAAT/enhancer binding protein α and CCAAT/enhancer binding protein β isoform synthesis in control and LPS-treated livers. Mol. Biol. Cell **9**, 1479–1494
47 Timchenko, N. A., Welm, A. L., Lu, X. and Timchenko, L. T. (1999) CUG repeat binding protein (CUGBP1) interacts with the 5′ region of C/EBPβ mRNA and regulates translation of C/EBPβ isoforms. Nucleic Acids Res. **27**, 4517–4525
48 Timchenko, L. T., Iakova, P., Welm, A. L., Cai, Z. J. and Timchenko, N. A. (2002) Calreticulin interacts with C/EBPα and C/EBPβ mRNAs and represses translation of C/EBP proteins. Mol. Cell. Biol. **22**, 7242–7257
49 Welm, A. L., Timchenko, N. A. and Darlington, G. J. (1999) C/EBPα regulates generation of C/EBPβ isoforms through activation of specific proteolytic cleavage. Mol. Cell. Biol. **19**, 1695–1704
50 Lichtsteiner, S. and Schibler, U. (1989) A glycosylated liver-specific transcription factor stimulates transcription of the albumin gene. Cell **57**, 1179–1187

Received 21 November 2005/20 March 2006; accepted 11 April 2006
Published as BJ Immediate Publication 11 April 2006, doi:10.1042/BJ20051863

Available online at www.sciencedirect.com
ScienceDirect
The International Journal of Biochemistry & Cell Biology 39 (2007) 171–180
IJBCB
www.elsevier.com/locate/biocel

Purification and characterization of C-terminal truncated forms of histone H2A in monocytic THP-1 cells

Jiro Minami [a,b], Koji Takada [a,*], Katsuhiko Aoki [a], Yohta Shimada [a], Yutaka Okawa [b], Noriko Usui [b], Kiyoshi Ohkawa [a]

[a] *Department of Biochemistry 1, Jikei University School of Medicine, 3-25-8, Nishishinbashi, Minato-ku, Tokyo 105-8461, Japan*
[b] *Division of Hematology and Oncology, Department of Internal Medicine, Jikei University School of Medicine, Tokyo, Japan*

Received 22 April 2006; received in revised form 20 July 2006; accepted 27 July 2006
Available online 18 August 2006

Abstract

Histones are key components of chromatin. We investigated histone H2A-immunoreactive proteins in acute monocytic leukemia THP-1 cells using three polyclonal antibodies raised against peptides corresponding to distinct regions of H2A. Two unknown immunoreactive proteins (9- and 12-kDa proteins), H2A (14 kDa) and ubiquitinated H2A (23 kDa) were found in the cell lysates prepared by immediate direct addition of SDS-PAGE sample buffer to the cells as well as in the nuclear and chromatin fractions. However, they were not found in the cytoplasmic fraction. The unknown proteins were successfully purified by immunoaffinity chromatography from the cell nucleus extract and identified as 9-kDa $H2A_{1-87}$ and 12-kDa $H2A_{1-114}$, suggesting that both were produced by limited proteolysis of intact $H2A_{1-129}$. The truncated forms of H2A probably persisted as chromatin constituents, since the stability of $H2A_{1-87}$ in the chromatin fraction was sensitive to treatment with micrococcal nuclease, and $H2A_{1-114}$ was solubilized with lower ionic strength from the chromatin fraction obtained by micrococcal nuclease treatment. Truncated H2A proteins in THP-1 cells were transiently increased in amount by short-term treatment with phorbol 12-myristate 13-acetate or all-*trans*-retinoic acid, both of which induce macrophage-like differentiation. Furthermore, these increases were suppressed by preceding treatment with carbobenzoxy-L-leucyl-L-leucyl-L-leucinal (MG132) but not with carbobenzoxy-L-isoleucyl-γ-*t*-butyl-L-glutamyl-L-alanyl-L-leucinal (PSI), both of which are generally known as proteasome inhibitors. Our results suggest that histone H2A is cleaved at least at two sites by protease(s) that remain obscure, and might affect chromatins in the early stage of THP-1 cell differentiation.

Keywords: Histone H2A; Proteolysis; Phorbol 12-myristate 13-acetate; MG132; THP-1 cell

1. Introduction

Histone proteins are factors that regulate chromatin functions. They act as acceptors for a variety of post-translational modifications, including acetylation, methylation and ubiquitination of lysine residues, methylation of arginine residues, and phosphorylation of serine and threonine residues (Peterson & Laniel, 2004). These modifications of the histone tails are involved in the regulation of replication, transcription and cell cycle progression (Cosgrove, Boeke, & Wolberger,

Abbreviations: RA, all-*trans*-retinoic acid; DMSO, dimethyl sulfoxide; FBS, fetal bovine serum; PMA, phorbol 12-myristate 13-acetate; PMSF, phenylmethylsulfonylfluoride; PVDF, polyvinilidene difluoride; TBS, Tris-buffered saline; ZLLal, carbobenzoxy-L-leucyl-L-leucinal

* Corresponding author. Tel.: +81 3 3433 1111x2226; fax: +81 3 3435 1922.
E-mail address: takada@jikei.ac.jp (K. Takada).

1357-2725/$ – see front matter © 2006 Elsevier Ltd. All rights reserved.
doi:10.1016/j.biocel.2006.07.010

2004; Peterson & Laniel, 2004; Turner, 2002). Exchange of histones and histone variants promoted by histone chaperones and other proteins are also implicated in some of these cellular processes (Chakravarthy, Park, Chodaparambil, Edayathumangalam, & Luger, 2005). Therefore, the state of the histones reflects the epigenetic events in mammalian cell nuclei.

Proteins can also be modified by proteolytic cleavage, a process involved in the maturation and regulation of various cellular proteins (Kidd, Lahti, & Teitz, 2000; Neurath, 1991). Chromatin-bound proteolytic activity, which cleaves histone H2A between Val_{114} and Leu_{115}, yielding $H2A_{1-114}$ and a free pentadecapeptide in the high ionic strength condition, has been found in calf thymus nuclei (Eickbush, Watson, & Moudrianakis, 1976). The enzyme catalyzing this cleavage has been partially purified and named H2A-specific protease (Davie, Numerow, & Delcuve, 1986; Eickbush et al., 1976). H2A-specific protease is selectively associated with H1-containing nucleosomes (Davie et al., 1986), and produces $H2A_{1-114}$ from acetylated histone octamer-DNA reconstituted in the physiological condition (Eickbush, Godfrey, Elia, & Moudrianakis, 1988) it may affect nucleosomal conformation since the cleavage of H2A lowers the binding affinity between the H2A:H2B dimer and the H3:H4 tetramer *in vitro* (Elia & Moudrianakis, 1988). However, fundamental properties of H2A-specific protease, including its primary structure and biological roles, remain obscure. Okawa et al. (2003) have recently purified two truncated forms of monoubiqutinated H2A from the nuclei of acute myeloid leukemia OCI/AML 1a cells, and found that the cellular levels of one of these compounds were changed by treatment with phorbol 12-myristate 13-acetate (PMA) or all-*trans*-retinoic acid (RA). However, whether or not the truncated form(s) of non-ubiquitinated H2A exist as well as the enzyme catalyzing these cleavages has remained obscure.

In the present study, using three anti-histone H2A antibodies that recognize different regions of H2A, we analyzed H2A-immunoreactive proteins in human acute monocytic leukemia THP-1 cells, and identified two truncated forms of H2A, which were presumably produced by H2A-specific protease and/or other protease(s).

2. Materials and methods

2.1. Cell culture

Cells of the acute monocytic leukemia cell line THP-1 were cultured in RPMI 1640 medium supplemented with 2 mM L-glutamine, 100 units/ml penicillin and streptomycin, and 10% fetal bovine serum at 37 °C and 5% CO_2. They were maintained by three passages per week. To induce macrophage-like differentiation, the cells were cultivated in the presence of 50 ng/ml PMA or 1 μM RA.

In experiments in which endogenous protease activities were inhibited, the cells were cultivated in the presence of the following additives: *o*-phenanthroline (Dojindo Laboratories, Kumamoto, Japan) as a metalloprotease inhibitor; carbobenzoxy-L-leucyl-L-leucinal (ZLLal) (Peptide Institute Inc., Osaka, Japan) as a calpain inhibitor; and carbobenzoxy-L-isoleucyl-γ-*t*-butyl-L-glutamyl-L-alanyl-L-leucinal (PSI) and carbobenzoxy-L-leucyl-L-leucyl-L-leucinal (MG132) from Peptide Institute Inc. as proteasome inhibitors.

2.2. Cell extraction

Unless otherwise stated, all procedures were performed under ice cooling or at 4 °C. The cells were harvested by centrifugation (300 × *g*, 10 min) with two washing steps in phosphate-buffered saline. For the preparation of whole cell extracts, a cell pellet derived from approximately 1×10^7 cells was lysed with 0.4 ml of SDS-PAGE sample buffer containing 50 mM Tris–HCl, pH 6.8, 2% SDS, 10% glycerol, 0.05% bromophenol blue, and 50 mM dithiothreitol and then heated at 100 °C for 3 min followed by brief sonication. In an experiment to evaluate artificial cleavage by the cell extraction procedure, bovine histone H2A (3 μg), which had been biotinylated using sulfosuccinimidyl-6-(biotinamido) hexanoate (Pierce, Rockford, IL), was added to the cell pellet (8×10^6 cells) prior to the addition of SDS-sample buffer.

For the preparation of nuclear extracts, a cell pellet (approximately 1×10^7 cells) was suspended in 1 ml of 10 mM Tris–HCl, pH 7.4, containing a protease inhibitor mixture consisting of 0.05% Nonidet P-40, 150 mM NaCl, 3 mM $MgCl_2$, 0.5 mM phenylmethylsulfonylfluoride (PMSF), 1 mM EDTA, 0.5 μM antipain, 1 μM aprotinin, 0.1 μM leupeptin, 35 μM chymostatin, 1 μM pepstatin A, 3 μM *trans*-epoxysuccinyl-L-leucylamido-(4-guanidino) butane, 0.5 mM benzamidine, 30 μM phosphoramidon and 0.1 mM bestatin, expressed as final concentrations. The suspension was briefly sonicated, then centrifuged at 1200 × *g* for 5 min, and the cytoplasmic supernatant subsequently discarded. From the resultant nuclear pellets, the chromatin fraction and nuclear proteins were prepared according to the methods described previously (Okawa et al., 2003).

2.3. Antibodies

Two distinct rabbit antisera recognizing histone H2A were prepared against synthetic peptides corresponding to residues 11–24 (RAKAKTRSSRAGLQ) and residues 70–81 (ARDNKKTRIIPR) of human histone H2A, respectively, with a cysteine added to the C-terminus. These peptides were coupled to keyhole limpet hemocyanin using 3-maleimidobenzoic acid *N*-hydroxysuccinimide ester (Pierce, Rockford, IL). Immunization using the multiple intradermal injections into rabbits was completed according to the method of Vaitukaitis (1981). These antisera were affinity-purified and named 2A11 and 2A70, respectively. In addition, the purified 2A11 antibody was covalently coupled to Sepharose using NHS-activated Sepharose (Amersham Biosciences, Uppsala, Sweden), and the 2A11-immobilized Sepharose was employed as a matrix for affinity chromatography.

Rabbit polyclonal antibody recognizing the carboxyl terminal region of human H2A (#sc-8648, named C19) was purchased from Santa Cruz Biotechnology (Santa Cruz, CA). Rabbit polyclonal antibodies against histone H4 (#07-108) and mouse monoclonal antibodies against histone H1 (#05-457) and H3 (#05-499) were purchased from Upstate Biotechnology (Lake Placid, NY). Anti-ubiquitin monoclonal antibody (Ab5F9) was prepared by some of the authors (Takada, Kanda, Ohkawa, & Matsuda, 1994).

2.4. Electrophoretic analyses

The subcellular proteins and protein samples were dissolved in the SDS-PAGE sample buffer, and resolved by SDS-PAGE on 16.5% acrylamide gels in Tris–tricine buffer (Schagger & von Jagow, 1987). The resolved proteins were transferred onto a nitrocellulose membrane (Kyhse-Andersen, 1984). The blotted membranes were blocked by 2 h-incubation in immunoblot buffer containing Tris-buffered saline (TBS), 0.05% Tween-20 with 0.1% gelatin and 0.1% casein. Immunostaining was performed by incubating the blots in each primary antibody at the appropriate dilution in the immunoblot buffer for 2 h. The blots were then washed four times with washing buffer (TBS containing 0.05% Tween-20) and incubated with secondary alkaline phosphatase conjugated anti-mouse or rabbit immunoglobulin Fab fragments (Nichirei Corp., Tokyo, Japan), and developed by the method of Leary, Brigati, and Ward (1983). In cases where histone H2A, H3, H4, and ubiquitin were detected prior to the blocking, the blots were autoclaved at 120 °C for 30 min to enhance the immunoreactivities to each antigen (Takada et al., 1994). Prestained molecular weight standards (BioRad, Hercules, CA) were used to monitor protein migration.

2.5. Affinity purification of H2A-immunoreactive proteins

Nuclei were obtained from approximately 3×10^8 THP-1 cells, and nuclear pellets were solubilized with 5 ml of SDS-PAGE sample buffer as described above. This mixture was centrifuged briefly to pellet insoluble debris, and diluted with 9 ml of buffer containing 40 mM Tris–HCl, pH 7.4, 200 mM NaCl, and 0.2% CHAPS. Removal of SDS from this solution was performed using SDS-OUT sodium dodecyl sulfate precipitation reagent (Pierce), and then the solution was dialyzed with Buffer A containing TBS, 0.1% CHAPS, 0.5 mM PMSF and 1 mM EDTA, followed by centrifugation at $100{,}000 \times g$ for 60 min. The resulting supernatant was applied to a 2A11-Sepharose column (1 ml of gel volume) and after washing with 5 ml of Buffer A, the column was developed with 6 ml of 50 mM Tris–HCl, pH 7.5, containing 3.5 M $MgCl_2$ and 0.1% CHAPS.

2.6. Enzymatic digestion of H2A-immunoreactive proteins

The fraction of the affinity-purified H2A-immunoreactive proteins was divided into two portions, one of which was subjected to reverse-phase HPLC on a capillary column (C18, 5 μm, 300 Å, 150 mm × 0.5 mm; Brownlee Columns, Perkin-Elmer) using the eluting conditions described previously (Okawa et al., 2003). The eluate containing 12-kDa protein was recovered and dried in a SpeedVac, dissolved in 50 μl of 20 mM Tris–HCl, pH 9.0, and incubated at 37 °C for 15 h with 0.3 pmol of endoproteinase Asp-N (Roche Diagnostics, Indianapolis, IN) to achieve enzymatic digestion. The digested peptides were resolved by reverse-phase HPLC under the conditions described above, and simultaneously deposited onto a polyvinilidene difluoride (PVDF) membrane using the 173A Microblotter apparatus (Applied Biosystems Inc., Foster City, CA) for further analyses.

The remaining fraction of the affinity-purified proteins was subjected to SDS-PAGE followed by Coomassie blue staining. The 9-kDa protein band was cut out from the gel and this gel piece then diced into 1 mm^3 fragments. These fragments were washed with 50 mM ammonium bicarbonate, pH 8.0, in 50% acetonitrile for 10 min, dried in a SpeedVac, and then added to 2 μl of 50 mM sodium phosphate, pH 7.8, containing 10 fmol of endoproteinase Asp-N. This solution was then

incubated on ice for 45 min. After the solution was fully absorbed, enzyme-free sodium phosphate was added until the gel fragments were covered, and the digestion was performed over-night at 37 °C followed by extraction with 5% trifluoroacetic acid in 50% acetonitrile with voltex for three times, and dried in vacuo.

2.7. Analyses of amino acid sequences and MS

Each of the proteins on the PVDF membranes was applied to an automated protein sequencer (model 492, Applied Biosystems) and the amino acid sequence analyzed. For MALDI-TOF-MS analysis, aliquots of matrix solution (1 μl each) of sinapinic acid (10 mg/ml in water) or α-cyano-4-hydroxycinnamic acid (10 mg/ml in 50% acetonitrile, 40% ethanol/0.1% trifluoroacetic acid) were applied to the target surface followed by the addition of 1 μl of each sample and drying under air. All spectra were recorded by the AXIMA-CFR (Shimadzu, Kyoto, Japan) in reflectron mode with the measurement range of 500–4000 *m/z* or in linear mode with the measurement range of 500–15,000 *m/z*.

2.8. RT-PCR

Total RNA was prepared from cells (2×10^6) using the SV Total RNA Isolation System (Promega, Madison, WI) according to the manufacturer's instructions. RT-PCR was carried out in a single tube (Sellner, Coelen, & Mackenzie, 1992). Each reaction contained 0.8 U transcriptor reverse transcriptase (Roche Diagnostics), 0.4 U Fast Start Taq DNA polymerase (Roche Diagnostics), 10 ng total RNA, 1 μl 10× PCR reaction buffer containing 20 mM $MgCl_2$, 400 μM dNTPs and 1 μM primers for each gene. The primer sequences were as follows: *c-fos*, 5′-TTGTGAAGAC CATGACAGGA GG-3′ and 5′-GATGCTCTTG ACAGGTTCCA CT-3′; *c-jun*, 5′-GATCCTGAAA CAGAGCATGA CC-3′ and 5′-AGTTGCTGAG GTTTGCGTAG AC-3′; Egr1, 5′-CCCCTCTGTC TACTATTAAG GC-3′ and 5′-GTTCATCGCTCCTGGCAAAC TT-3′. The tubes were incubated and thermal cycled (30 min at 55 °C, 4 min at 95 °C, then 25 cycles of 95 °C for 30 s, 55 °C for 30 s and 72 °C for 30 s) using the GeneAmp PCR System 9700 (Applied Biosystems).

3. Results

3.1. Immunochemical detection of putative truncated forms of histone H2A

In order to analyze histone H2A in THP-1 cells, we employed three distinct antibodies, named 2A11, 2A70 and C19, which were raised against different regions of H2A (Fig. 1A). To avoid artificial degradation as much as possible, the cell extracts were prepared by the immediate addition of SDS-PAGE sample buffer to the collected cells and then subjected to Western blotting with these antibodies (Fig. 1B). The 2A11 antibody recognizing the adjacent region of the N-terminus H2A (residues 11–24) markedly immunostained four bands at molecular masses of 9, 12, 14 and 23 kDa. The 23-kDa band was also detected by the 2A70 antibody recognizing the cen-

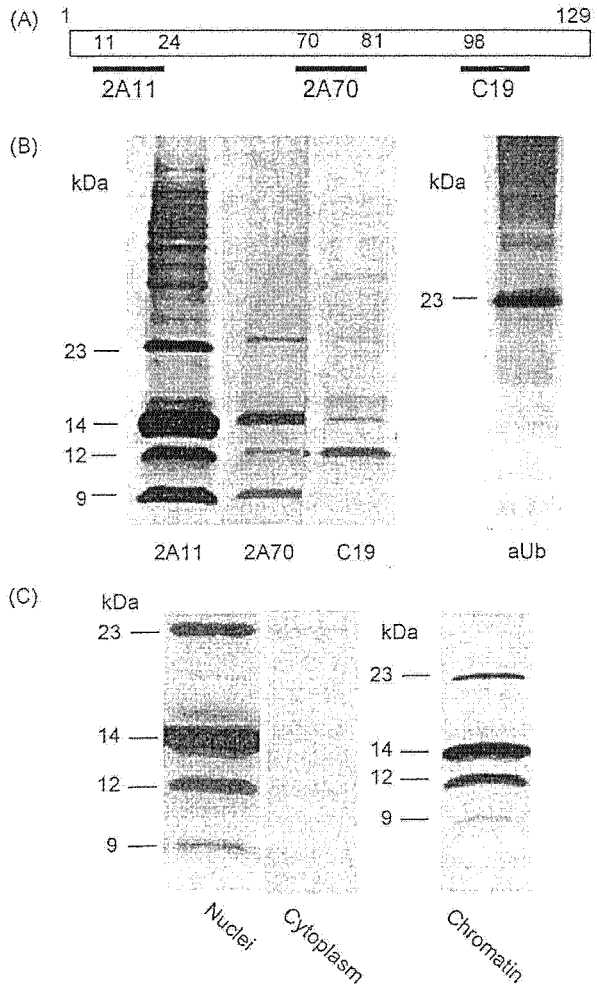

Fig. 1. Detection of histone H2A-immunoreactive proteins. (A) Regions of synthetic peptides used as antigens (2A11 and 2A70) or a blocking peptide provided by the supplier (C19). The antibodies of 2A11 and 2A70 recognize $H2A_{11-24}$ and $H2A_{70-81}$, respectively, and the C19 antibody recognizes the carboxyl terminal region. (B) Whole cell extracts of THP-1 cells containing proteins (15 μg each) were subjected to SDS-PAGE followed by immunoblotting using anti-H2A antibodies (2A11, 2A70 and C19) and anti-ubiquitin antibody (aUb). (C) Subcellular localization of the H2A-immunoreactive proteins detected by the antibody 2A70. Nuclear and cytoplasmic fractions (5 μg each) and a part of the chromatin fraction were applied to SDS-PAGE followed by immunoblotting.

tral region of H2A (residues 70–81) and anti-ubiquitin antibody (Fig. 1B), suggesting that it corresponded to mono ubiquitinated H2A. The 14-kDa band, which was detected by all three H2A antibodies, was estimated to be intact H2A since the theoretical mass of human H2A.1 was also calculated to be 13,960 kDa. The 12-kDa band was also immunostained by all three antibodies. The 9-kDa band was visualized by 2A11 and 2A70 antibodies, but not detected by C19 antibody which recognizes the neighboring region of the C-terminus. Judging from their sizes, we predicted that the 9- and 12-kDa proteins were truncated forms of H2A.

To clarify subcellular localization of the H2A-immunoreacitive proteins, the fractions of nuclei, cytoplasm and chromatin were subjected to Western blot analysis. The 9-, 12-, 14-, and 23-kDa proteins were found in the nuclear and chromatin fractions, but not in the cytoplasmic fraction (Fig. 1C).

The location of these H2A-immunoreactive proteins was further investigated using the nuclear fractionation procedure. The nuclei of THP-1 cells were incubated with or without micrococcal nuclease for 30 min. This treatment with micrococcal nuclease digested nuclear DNA, which was released as mono- and oligonucleosomal fragments (data not shown). Each nucleus was extracted in various concentrations of NaCl, and the S_0, S_1, S_2, and P fractions thus obtained were analyzed by SDS-PAGE followed by Western blotting using the 2A70 antibody. Without micrococcal nuclease digestion, the 9-, 12- and 14-kDa proteins were predominantly localized to the insoluble P fraction (Fig. 2A). The nuclease digestion induced release of the 12- and 14-kDa proteins since both band intensities in the S_1 and S_2 fractions were increased (Fig. 2B). These results suggest that the 12- and 14-kDa proteins bind to chromatins, most of which are sensitive to micrococcal nuclease, and thus

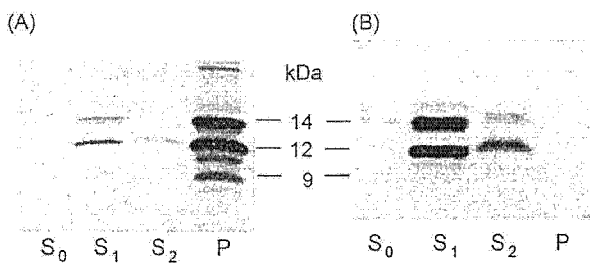

Fig. 2. Histone H2A-immunoreactive proteins in salt-fractionated chromatins of THP-1 cells. Nuclei, treated without (A) or with (B) micrococcal nuclease, were extracted with increasing salt (sodium chloride) concentrations as follows: 0 M (S_0), 1 M (S_1), 2 M (S_2) and insoluble residue (P). Details of the method have been described previously [11]. Proteins (3 μg each) in the samples were subjected to SDS-PAGE followed by immunoblotting using antibody 2A70.

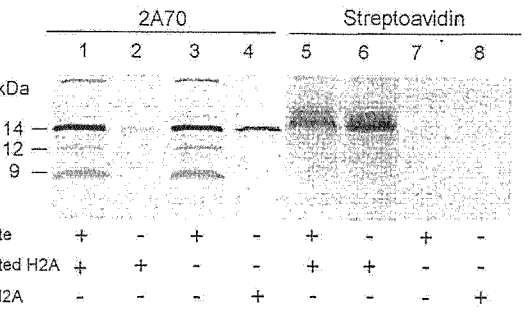

Fig. 3. Detection of H2A-immunoreactive proteins and biotinylated H2A. Sample mixtures with (+) or without (−) cell lysates (whole cell extracts containing 15 μg of proteins), biotinylated H2A (20 ng) and bovine H2A (100 ng) were subjected to SDS-PAGE, and transferred to nitrocellulose membranes. Lanes from 1 to 4 and from 5 to 8 were probed with the 2A70 antibody and streptoavidin conjugated with alkaline phosphatase.

they can be solubilized with lower ionic strength. The 9-kDa protein became undetectable as a result of the nuclease digestion (Fig. 2A and B) suggesting that this protein may be sensitive to proteolytic activities released by the nuclease treatment.

In order to assess the influence of the cell extraction procedure on the appearance of putative H2A truncated forms, biotinylated H2A was added to THP-1 cells followed by direct lysis in SDS-PAGE sample buffer. Biotinylated H2A was not truncated by the lysis procedure (Fig. 3), suggesting that the 9- and 12-kDa proteins are not produced artificially during cell extraction.

3.2. *Purification and identification of the H2A-immunoreactive proteins*

Immunoaffinity chromatography using 2A11 antibody-immobilized Sepharose was employed to isolate the 9- and 12-kDa proteins. The nuclear extract, containing 64 mg of proteins, was applied to the 2A11-Sepharose column. The great majority of proteins did not bind to the column, whereas a small amount (0.23 mg of the proteins) was adsorbed and recovered as the $MgCl_2$ eluate. SDS-PAGE followed by silver staining revealed that the eluate contained four bands of 9, 12, 14, and 23 kDa, respectively (Fig. 4A). These bands were immunostained with the three antibodies against histone H2A (Fig. 4B), indicating that the H2A-immunoreactive proteins were purified successfully.

The $MgCl_2$ eluate was further fractionated by reverse-phase HPLC with the result that the 12-kDa protein was isolated to homogeneity (data not shown). The 12-kDa protein was then digested by endoproteinase Asp-N, and analyzed again by reverse-phase

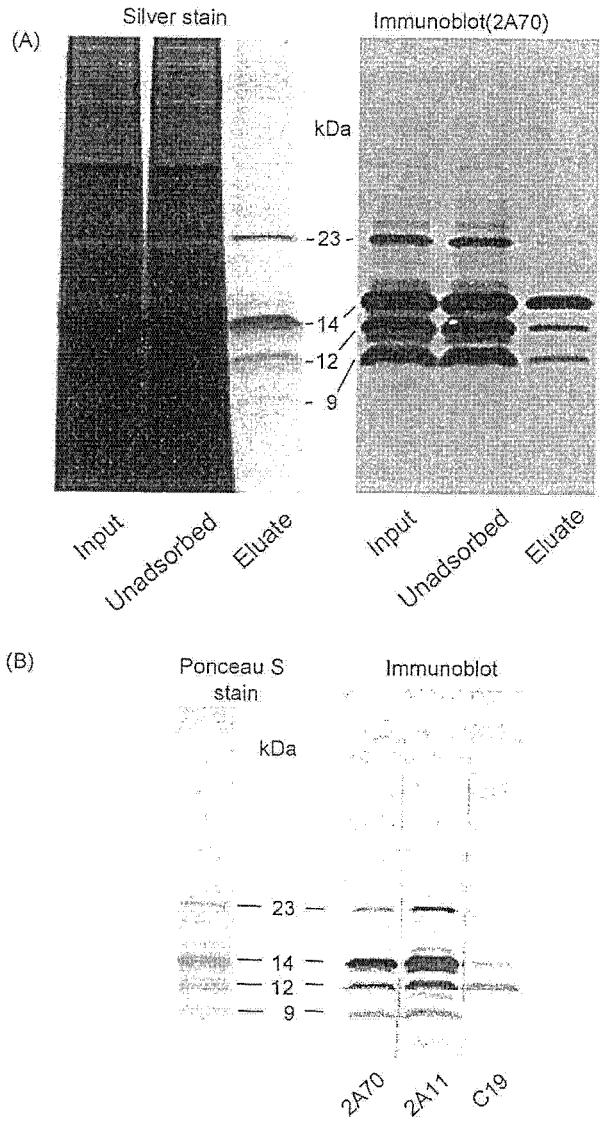

Fig. 4. Proteins and H2A-immunoreactive proteins in fractions from immunoaffinity chromatography. A nuclear extract (Input) was applied to the column, and the unbound run-through fraction (Unadsorbed) and bound-eluted fraction (Eluate) were collected. (A) Proteins of each fraction were subjected to SDS-PAGE, and visualized by silver staining, or followed by immunoblotting using antibody 2A70. The loaded amounts were adjusted in the same volume proportion of each fraction. (B) Proteins of the "Eluate" fraction were subjected to SDS-PAGE and transferred to nitrocellulose membranes, followed by staining with Ponceau S or by immunostaining using three antibodies (2A70, 2A11 and C19) against H2A.

HPLC (Fig. 5). Edman degradation analysis of the resulting digests led to determination of the amino acid sequences of the following two peptide fragments: peak 1: DNK-TRIIP-HL, and peak 2: DEELNKLL-GKVTIAQGGVLPNIQ, corresponding to residues 72–83 and 90–112 of H2A, respectively (Fig. 6). From

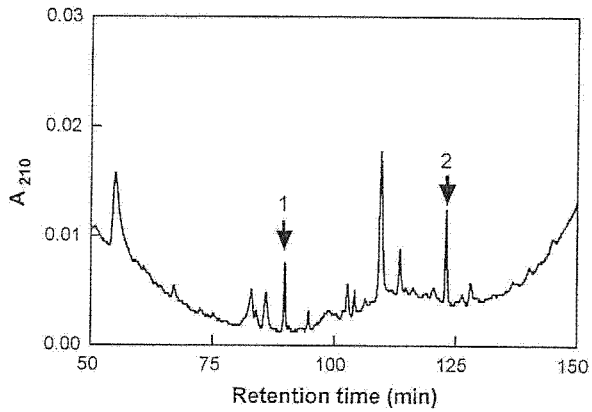

Fig. 5. Reverse-phase HPLC of endoproteinase Asp-N-digested peptide fragments obtained from the 12-kDa protein. The 12-kDa protein purified to homogeneity by the immunoaffinity chromatography followed by reverse-phase HPLC was subjected to limited proteolysis and applied to a capillary column for reverse-phase HPLC. Absorbance at 210 nm was then monitored. Peaks eluted with a gradient of acetonitrile, and two peptide peaks (1 and 2) were separately collected, and subjected to Edman degradation analysis.

all of the other peaks in the chromatogram (Fig. 5), no sequence data were obtained, possibly because of peptide N-terminal modifications or nonpeptide contaminants. Molecular mass values determined by means of MALDI-TOF-MS were 12,320 Da for the 12-kDa protein, 2186.4 Da for peak 1 and 2619.2 Da for peak 2. These values were in good agreement with the calculated masses of N-terminal acetylated $H2A_{1-114}$ (12,319 Da) and the endoproteinase Asp-N-digested H2A fragments (2186.3 Da for $H2A_{72-89}$ and 2619.5 Da for $H2A_{90-114}$), respectively. From these results and the fact that H2A is acetylated at its N-terminal (Sautiere et al., 1974), the 12-kDa protein was identified as C-terminal truncated H2A (Δ 115–129), $H2A_{1-114}$.

For further analysis of the 9-kDa protein, a Coomassie-stained gel band was used as a source of the protein, since the 9-kDa protein bound irreversibly to the reverse-phase HPLC column and never eluted. The portion of the gel containing the 9-kDa protein band was incubated with endoproteinase Asp-N, and the digest mixture was extracted. This mixture was directly analyzed by Edman degradation, yielding a major sequence of DNKKTRIIPRHLQ, which shows complete identity to $H2A_{72-84}$. Furthermore, in the mixture, we found two constituents whose molecular mass values were determined to be 9446.6 Da and 1917.6 Da by MALDI-TOF-MS analysis, and these values were in good agreement with the calculated masses of N-terminal acetylated $H2A_{1-87}$ (9446.5 Da) and $H2A_{72-87}$ (1917.8 Da). These results indicate that the 9-kDa protein is another truncated form (Δ 88–129) of H2A, $H2A_{1-87}$.

Histone H2A.1

```
1         10        20        30        40        50        60        70
Ac- SGRGKQGGKARAKAKTRSSRAGLQFPVGRVHRLLRKGNYAERVGAGAPVYLAAVLEYLTAEILELAGNAA

          80        90        100       110       120       130
RDNKKTRIIPRHLQLAIRNDEELNKLLGKVTIAQGGVLPNIQAVLLPKKTESHHKAKGK
```

Peak 1 Peak 2

DNK-TRIIP-HL. DEELNKLLGKVTIAQGGVLPNIQ.

A fragment of the 9-kDa protein

DNKKTRIIPRHLQ.

Fig. 6. Determined amino acid sequences. Sequences determined by Edman degradation of endoproteinase Asp-N digests of 12-kDa protein and 9-kDa protein. The digest of the 12-kDa protein was fractionated by reverse-phase HPLC, and the resulting peaks 1 and 2 (Fig. 5) were analyzed. The digested 9-kDa protein was directly analyzed without further fractionation. Names of the samples are shown in bold-face. Sequences are given in one-letter codes below the sequence of H2A.1. Sequences not identified are indicated by dashes, and the dots at the end of the sequences indicate that the amino acid has not been determined from this point or that the analysis was terminated at this point since the resulting sequence was sufficient for the database search.

3.3. PMA and RA induced changes in levels of the truncated H2A

Acute monocytic leukemia THP-1 cells were differentiated to macrophage-like cells by cultivation in the presence of PMA and RA. H2A-immunoreactive proteins in the cells treated with PMA or RA were analyzed by Western blotting using the 2A70 antibody (Fig. 7). H2A (14 kDa) and the amounts of mono-ubiquitinated H2A (23 kDa) were not changed by treatment with either PMA or RA. However, $H2A_{1-87}$ (9 kDa) and $H2A_{1-114}$ (12 kDa) were transiently increased in amount by both treatments. These results suggest that truncation of H2A was accelerated in the early stage of differentiation of THP-1 cells.

3.4. Effects of protease inhibitors on appearance of the truncated H2A

Four different protease inhibitors were tested for their ability to inhibit the truncation of H2A. PMA-induced changes in levels of the truncated forms ($H2A_{1-87}$ and $H2A_{1-114}$) were observed to varying degrees in cells treated with ZLLal, *o*-phenanthroline, or PSI, whereas these changes were completely suppressed by treatment with MG132 (Fig. 8). These results suggest that MG132-sensitive protease may be involved in the truncation of H2A by short-term exposure to PMA.

$H2A_{1-87}$ and $H2A_{1-114}$ were transiently increased within 30 min after treatment with PMA and RA (Fig. 7). We predicted that H2A processing might be implicated in expression of the early response genes, such as *c-jun*, *c-fos*, and Egr-1, whose transcription is up-regulated under similar conditions (Akuzawa, Kurabayashi, Ohyama, Arai, & Nagai, 2000; Auwerx, Staels, & Sassone-Corsi, 1990). The amounts of mRNA of *c-jun*, *c-fos* and Egr-1 were apparently increased by PMA treatment in our experiment, however pre- and co-treatment with MG132 did not suppress the enhancement of expression of these genes (data not shown). Thus cleavage of histone H2A

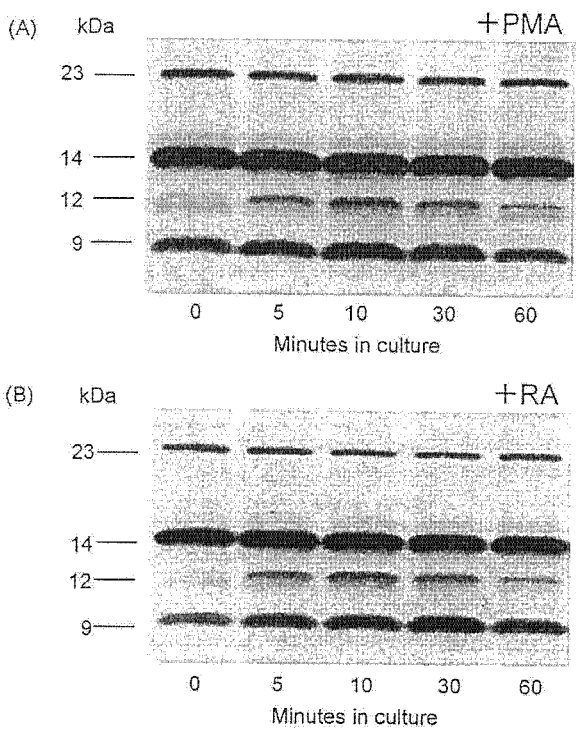

Fig. 7. Changes in the levels of H2A-immunoreactive proteins in THP-1 cells treated with phorbol 12-myristate 13-acetate (PMA) (A) or all-*trans*-retinoic acid (RA) (B). The cells were cultured in the presence of 50 ng/ml PMA or 1 μM RA for the indicated minutes. Proteins (15 μg each) of whole cell extracts were subjected to SDS-PAGE followed by immunoblotting using the 2A70 antibody recognizing H2A.

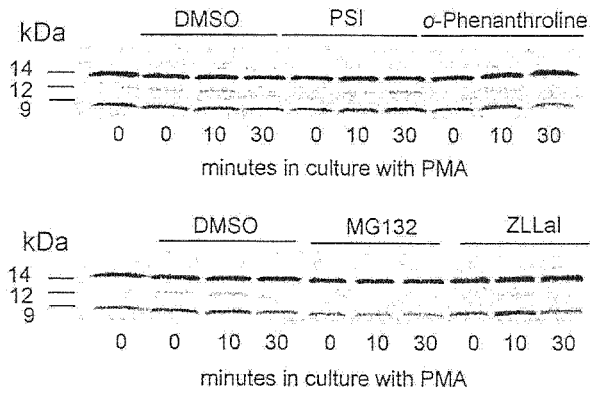

Fig. 8. Changes in the levels of H2A-immunoreactive proteins in THP-1 cells treated with phorbol 12-myristate 13-acetate (PMA) in the preceding culture with protease inhibitors. The cells were cultured for 2 h in the presence of dimethyl sulfoxide (DMSO) (0.1%), PSI (10 μM), *o*-phenanthroline (100 μM), MG132 (10 μM) and carbobenzoxy-L-leucyl-L-leucinal (ZLLal) (10 μM), and then PMA (50 ng/ml as the final concentration) was added to each cell for extended culture for up to 30 min. Proteins (15 μg each) of the whole cell extracts were subjected to SDS-PAGE followed by immunoblotting using the 2A70 antibody recognizing H2A.

might not contribute to an immediate response of the early response genes to PMA.

4. Discussion

In the present study, we found two H2A-immunoreactive proteins (9- and 12-kDa proteins) in human leukemia cell nuclei, and then purified and identified them as truncated forms of H2A, both of which were localized in the chromatin fraction (Fig. 1). We predict that H2A undergoes proteolytic cleavage at I_{87} and V_{114}, yielding $H2A_{1-87}$ (9 kDa) and $H2A_{1-114}$ (12 kDa), respectively (Fig. 9). On the other hand, the residual cleaved fragments corresponding to the C-terminal

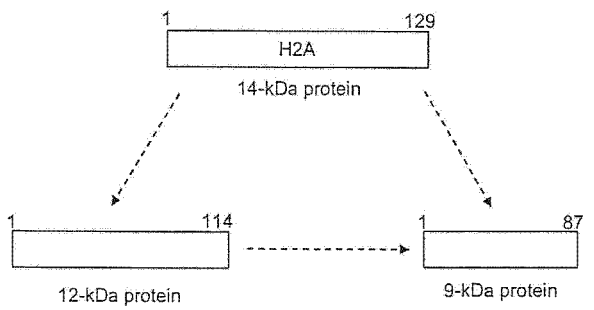

Fig. 9. A model for production of the truncated forms of histone H2A. $H2A_{1-114}$ (12 kDa) and $H2A_{1-87}$ (9 kDa) were found in the chromatin fraction of THP-1 cells. Native H2A (14 kDa) is cleaved by putative H2A-specific protease (Eickbush et al., 1976), forming $H2A_{1-114}$. In addition, unknown protease may produce $H2A_{1-87}$ by the processing of H2A or $H2A_{1-114}$.

region of H2A, i.e. $H2A_{115-129}$ (1683 Da), $H2A_{88-129}$ (4556 Da), and $H2A_{88-114}$ (2873 Da), were not detected in any of the nuclear samples tested by Western blot analysis using C19 antibody, even though the employed SDS-PAGE system showed good resolution in the 2–30 kDa range (Schagger & von Jagow, 1987), and the C19 antibody recognized this region (Fig. 1). These results suggest that the cleaved C-terminal fragments are not retained in the chromatin and thus subjected to degradation. Proteolytic degradation of histones including H1, H3, H2A and others, can occur during the preparation of chromatin from leukemic cells (Simpkins & Mahon, 1977). However, in the cell extracts prepared by direct lysis in SDS-PAGE sample buffer (same samples used in Fig. 7), no degraded bands were detected by Western blot analysis using each of the antibodies against H1, H3 and H4 (data not shown). In addition, the truncated forms were not produced from biotinylated H2A, which was exogenously added to the cells (Fig. 3). These results indicate that H2A, but probably not other histone proteins, undergoes endogenous limited proteolysis in the nuclei of THP-1 cells, by which we found the two truncated forms of H2A.

A 12.5-kDa proteolytic product of H2A has been found in acute leukemia cells, and the amount of this product in HL-60 cells is increased by treatment with DMSO, inducing differentiation of the cells (Pantazis, Sarin, & Gallo, 1981). Interestingly, our results indicate that the two truncated H2A levels in THP-1 cells were transiently increased by treatment with differentiation-inducing reagents (Fig. 7), and 9- and 12-kDa H2A-immunoreactive proteins were also found in acute myeloid leukemia OCI/AML 1a cells (data not shown). Therefore, the 12.5-kDa protein (Pantazis et al., 1981) conceivably was identical to the 12-kDa truncated H2A ($H2A_{1-114}$) in this study. $H2A_{1-114}$ production has been characterized *in vitro* by using fractions of H2A-specific protease prepared from calf thymus and liver (Davie et al., 1986; Eickbush et al., 1988; Eickbush et al., 1976; Elia & Moudrianakis, 1988). These studies clarified some aspects of this protease, but no direct evidence has been obtained to show that H2A is processed by the protease *in vivo*. Therefore, the 12-kDa truncated H2A detected immunochemically in the present study may be the first observation indicating the presence of the product ($H2A_{1-114}$) of the H2A-specific protease. To the best of our knowledge, $H2A_{1-87}$ is a novel processing product of H2A, which has lost the C-terminal region containing 42 amino acid residues.

Levels of the two truncated forms of H2A were transiently increased by short-term exposure of PMA and RA, but a concomitant decrease in the amounts of H2A

was not observed. Therefore, the source of $H2A_{1-87}$ and $H2A_{1-114}$ is unclear (Fig. 7). Another candidate of the source is ubiquitinated H2A, since the ubiquitin-H2A conjugate can also be cleaved by the H2A-specific protease (Davie et al., 1986); and 10-kDa ubiquitinated $H2A_{115-129}$, the product of ubiquitinated H2A processing, is found in leukemia cells (Okawa et al., 2003). However, during exposure (up to 1 h) to PMA and RA, levels of ubiquitinated H2A were almost stable (Fig. 7), and the cleaved fragments of ubiquitin-H2A conjugates (ubiquitinated $H2A_{115-129}$ or $H2A_{88-129}$) were not observed by Western blot analysis with anti-ubiquitin antibody (data not shown). One of the possible explanations of this discrepancy is that only a small part of the nucleosomal H2A is cleaved under the effect of PMA or RA, thus the consumption of H2A is negligible. It must be noted that the band intensities in the same lane of Fig. 7 are not precisely reflected in the amounts of these H2A forms, and anti-H2A antibody 2A70 is probably more reactive to the truncated forms than native H2A.

The increase in amounts of both truncated H2A resulting from PMA and RA treatment was effectively suppressed by only MG132, a well-known proteasome inhibitor (Tsubuki, Saito, Tomioka, Ito, & Kawashima, 1996) suggesting that MG132 exerts inhibitory activities against the protease(s) producing $H2A_{1-87}$ and $H2A_{1-114}$ (Fig. 8). However, it is unlikely that proteasome is involved in the limited proteolysis of such small protein like H2A. In addition, PSI, another proteasome inhibitor, was not effective in this experiment (Fig. 8), and MG132 has a wide inhibitory spectrum against various proteases, such as calpain (Tsubuki et al., 1996) and cathepsin K (Votta et al., 1997). Therefore, MG132 may affect protease(s) other than proteasome, which cleaves H2A such as the H2A-specific protease. To obtain a clear understanding of the targets of MG132, identification of the protease responsible for the processing of H2A should be pinpointed.

A fundamental question is: "What is the role of the limited proteolysis of H2A in chromatin of THP-1 cells and other leukemic cells (Pantazis et al., 1981)?". The $H2A_{1-114}$ molecule still forms a stable H2A:H2B dimer, but the $H2A_{1-114}$:H2B dimer has a significantly reduced affinity constant for H3:H4 tetramer compared to native dimer, suggesting that this proteolysis leads to a more extended nucleosomal conformation, which may facilitate transcription or replication (Elia & Moudrianakis, 1988). In this context, the PMA/RA-induced transient increases in $H2A_{1-87}$ and $H2A_{1-114}$ (Fig. 7) might be involved in transcription in the early stage of differentiation. However, MG132 treatment, which can suppress these increases in the truncated forms of H2A (Fig. 8), could not prevent PMA-induced expression of the early response genes (data not shown). Considering the wide inhibitory spectrum of MG132, it is difficult to draw any definite conclusion, and thus the significance of H2A truncation remains controversial. More highly specific inhibition of H2A processing, using for example siRNA for the responsible protease, will be needed to obtain further insight into the limited proteolysis of histone H2A.

Acknowledgements

We are grateful to Ms. Sayako Takahashi and Ms. Tae Hirakawa for supporting our experiments. We also thank Prof. Masayuki Kobayashi (Internal Medicine, Jikei University School of Medicine) for his helpful advice.

References

Akuzawa, N., Kurabayashi, M., Ohyama, Y., Arai, M., & Nagai, R. (2000). Zinc finger transcription factor Egr-1 activates Flt-1 gene expression in THP-1 cells on induction for macrophage differentiation. *Arteriosclerosis, Thrombosis, and Vascular Biology, 20*, 377–384.

Auwerx, J., Staels, B., & Sassone-Corsi, P. (1990). Coupled and uncoupled induction of fos and jun transcription by different second messengers in cells of hematopoietic origin. *Nucleic Acids Research, 18*, 221–228.

Chakravarthy, S., Park, Y. J., Chodaparambil, J., Edayathumangalam, R. S., & Luger, K. (2005). Structure and dynamic properties of nucleosome core particles. *FEBS Letters, 579*, 895–898.

Cosgrove, M. S., Boeke, J. D., & Wolberger, C. (2004). Regulated nucleosome mobility and the histone code. *Nature Structural and Molecular Biology, 11*, 1037–1043.

Davie, J. R., Numerow, L., & Delcuve, G. P. (1986). The nonhistone chromosomal protein, H2A-specific protease, is selectively associated with nucleosomes containing histone H1. *The Journal of Biological Chemistry, 261*, 10410–10416.

Eickbush, T. H., Godfrey, J. E., Elia, M. C., & Moudrianakis, E. N. (1988). H2a-specific proteolysis as a unique probe in the analysis of the histone octamer. *The Journal of Biological Chemistry, 263*, 18972–18978.

Eickbush, T. H., Watson, D. K., & Moudrianakis, E. N. (1976). A chromatin-bound proteolytic activity with unique specificity for histone H2A. *Cell, 9*, 785–792.

Elia, M. C., & Moudrianakis, E. N. (1988). Regulation of H2a-specific proteolysis by the histone H3:H4 tetramer. *The Journal of Biological Chemistry, 263*, 9958–9964.

Kidd, V. J., Lahti, J. M., & Teitz, T. (2000). Proteolytic regulation of apoptosis. *Seminars in Cell and Developmental Biology, 11*, 191–201.

Kyhse-Andersen, J. (1984). Electroblotting of multiple gels: A simple apparatus without buffer tank for rapid transfer of proteins from polyacrylamide to nitrocellulose. *Journal of Biochemical and Biophysical Methods, 10*, 203–209.

Leary, J. J., Brigati, D. J., & Ward, D. C. (1983). Rapid and sensitive colorimetric method for visualizing biotin-labeled DNA probes hybridized to DNA or RNA immobilized on nitrocellulose: Bio-

blots. *Proceedings of the National Academy of Sciences of the United States of America, 80*, 4045–4049.

Neurath, H. (1991). Proteolytic processing and regulation. *Enzyme, 45*, 239–243.

Okawa, Y., Takada, K., Minami, J., Aoki, K., Shibayama, H., & Ohkawa, K. (2003). Purification of N-terminally truncated histone H2A-monoubiquitin conjugates from leukemic cell nuclei: Probable proteolytic products of ubiquitinated H2A. *The International Journal of Biochemistry and Cell Biology, 35*, 1588–1600.

Pantazis, P., Sarin, P. S., & Gallo, R. C. (1981). Detection of a histone-2A related polypeptide in differentiated human myeloid cells (HL-60) and its distribution in human acute leukemia. *International Journal of Cancer, 27*, 585–592.

Peterson, C. L., & Laniel, M. A. (2004). Histones and histone modifications. *Current Biology, 14*, R546–R551.

Sautiere, P., Tyrou, D., Laine, B., Mizon, J., Ruffin, P., & Biserte, G. (1974). Covalent structure of calf-thymus ALK-histone. *European Journal of Biochemistry, 41*, 563–576.

Schagger, H., & von Jagow, G. (1987). Tricine-sodium dodecyl sulfate-polyacrylamide gel electrophoresis for the separation of proteins in the range from 1 to 100 kDa. *Analytical Biochemistry, 166*, 368–379.

Sellner, L. N., Coelen, R. J., & Mackenzie, J. S. (1992). A one-tube one manipulation RT-PCR reaction for detection of Ross River virus. *Journal of Virological Methods, 40*, 255–264.

Simpkins, H., & Mahon, K. (1977). The histone content of chromatin preparations from leukaemic cells. *British Journal of Haematology, 37*, 467–473.

Takada, K., Kanda, T., Ohkawa, K., & Matsuda, M. (1994). Ubiquitin and ubiquitin-protein conjugates in PC12h cells: Changes during neuronal differentiation. *Neurochemical Research, 19*, 391–398.

Tsubuki, S., Saito, Y., Tomioka, M., Ito, H., & Kawashima, S. (1996). Differential inhibition of calpain and proteasome activities by peptidyl aldehydes of di-leucine and tri-leucine. *The Journal of Biochemistry, 119*, 572–576.

Turner, B. M. (2002). Cellular memory and the histone code. *Cell, 111*, 285–291.

Vaitukaitis, J. L. (1981). Production of antisera with small doses of immunogen: Multiple intradermal injections. *Methods in Enzymology, 73*(Pt B), 46–52.

Votta, B. J., Levy, M. A., Badger, A., Bradbeer, J., Dodds, R. A., James, I. E., et al. (1997). Peptide aldehyde inhibitors of cathepsin K inhibit bone resorption both in vitro and in vivo. *The Journal of Bone and Mineral Research, 12*, 1396–1406.

Artificial Organs
31(2):148–170, Blackwell Publishing, Inc.

Thoughts and Progress

Extracorporeal Bioartificial Liver Using the Radial-flow Bioreactor in Treatment of Fatal Experimental Hepatic Encephalopathy

*Hideki Kanai, *¶Hideki Marushima, †Naofumi Kimura, ‡Takamasa Iwaki, §Masaya Saito, ¶Haruka Maehashi, ¶Keiko Shimizu, ¶Makiko Muto, ¶Takahiro Masaki, ¶Kiyoshi Ohkawa, §Keitaro Yokoyama, §Masaaki Nakayama, **Tohru Harada, **Hiroshi Hano, ††Yoshiaki Hataba, ‡‡Takahiro Fukuda, ¶¶Masahiko Nakamura, ¶¶Naoto Totsuka, ¶¶Shutaro Ishikawa, *Yasuki Unemura, *Yuji Ishii, *Katsuhiko Yanaga, and §§Tomokazu Matsuura

*Department of Surgery, †Department of Pharmacology II, ‡Laboratory Animal Facilities, §Department of Internal Medicine, ¶Department of Biochemistry I, **Department of Pathology, ††Institute of DNA Medicine, ‡‡Department of Neuroscience, §§Department of Laboratory Medicine, The Jikei University School of Medicine, Tokyo, and ¶¶Biott Co. Ltd., Tokyo, Japan

Abstract: An extracorporeal bioartificial liver (BAL) that could prevent death from hepatic encephalopathy in acute hepatic insufficiency was aimed to develop. A functional human hepatocellular carcinoma cell line (FLC-4) was cultured in a radial-flow bioreactor. The function of the BAL was tested in mini-pigs with acute hepatic failure induced by α-amanitin and lipopolysaccharide. When the BAL system was connected with cultured FLC-4 to three pigs with hepatic dysfunction, all demonstrated electroencephalographic improvement and survived. Relatively low plasma concentrations of S-100 β protein, as a marker of astrocytic damage, from pigs with hepatic failure during BAL therapy were noted. BAL therapy can prevent irreversible brain damage from hepatic encephalopathy in experimental acute hepatic failure. **Key Words:** Acute hepatic failure—Radial-flow bioreactor—Cerebral edema—Astrocytes—α-Amanitin.

doi:10.1111/j.1525-1594.2007.00354.x

Received September 2005; revised July 2006.

Address correspondence and reprint requests to Dr. Tomokazu Matsuura, Department of Laboratory Medicine, The Jikei University School of Medicine, 3-25-8 Nishi-shinbashi, Minato-ku, Tokyo 105-8461, Japan. E-mail: matsuurat@jikei.ac.jp

A clinically effective bioartificial liver (BAL) requires development of a high-density cell culture module and a highly functioning liver cell line. We sought to develop a high-performance BAL to avoid lethal hepatic encephalopathy in acute hepatic insufficiency and establish the BAL as an extracorporeal circulation therapy able to surpass conventional blood purification procedures. Our extracorporeal BAL support system used a highly functional human hepatocellular carcinoma (HCC) cell line (FLC-4) cultured in a radial-flow bioreactor (RFB) (1,2). The RFB is packed with cell-adhesion scaffolds in a cylindrical array (Fig. 1A,B). The culture medium or the plasma flows from the periphery of the cylindrical module to the center. One important problem when cells are cultured densely is delivery of sufficient oxygen and nutrients even when these are plentiful at the inflow site. As a result, we could culture cells successfully at a density of 10^8/mL.

We have currently tested the BAL in mini-pigs with acute hepatic failure induced by α-amanitin, a mushroom-derived poison, and lipopolysaccharide (LPS), while monitoring with electroencephalography (EEG) to assess the effectiveness of BAL against hepatic encephalopathy. We measured the plasma levels of S-100 β protein, a marker of damage to astrocytes (3).

MATERIALS AND METHODS

Mini-pigs and monitoring

Male mini-pigs (CSK-MS) weighing 10–15 kg were a generous gift from Chugai Pharmaceutical (Tokyo, Japan). Prior to the experiments, they were maintained for 1–4 weeks at the Laboratory Animal Facilities of the Jikei University School of Medicine, receiving standard chow and water ad libitum. The study was approved by the institution's committee concerning animal experimentation.

Acute hepatic failure model

During inhalation anesthesia with 3–4% isoflurane, 0.05 mg/kg of α-amanitin (Calbiochem, Darmstadt, Germany) and 1 μg/kg of LPS (Sigma, St. Louis, MO, USA) dissolved in 10 mL of saline was administered via the splenic vein. Fifty percent

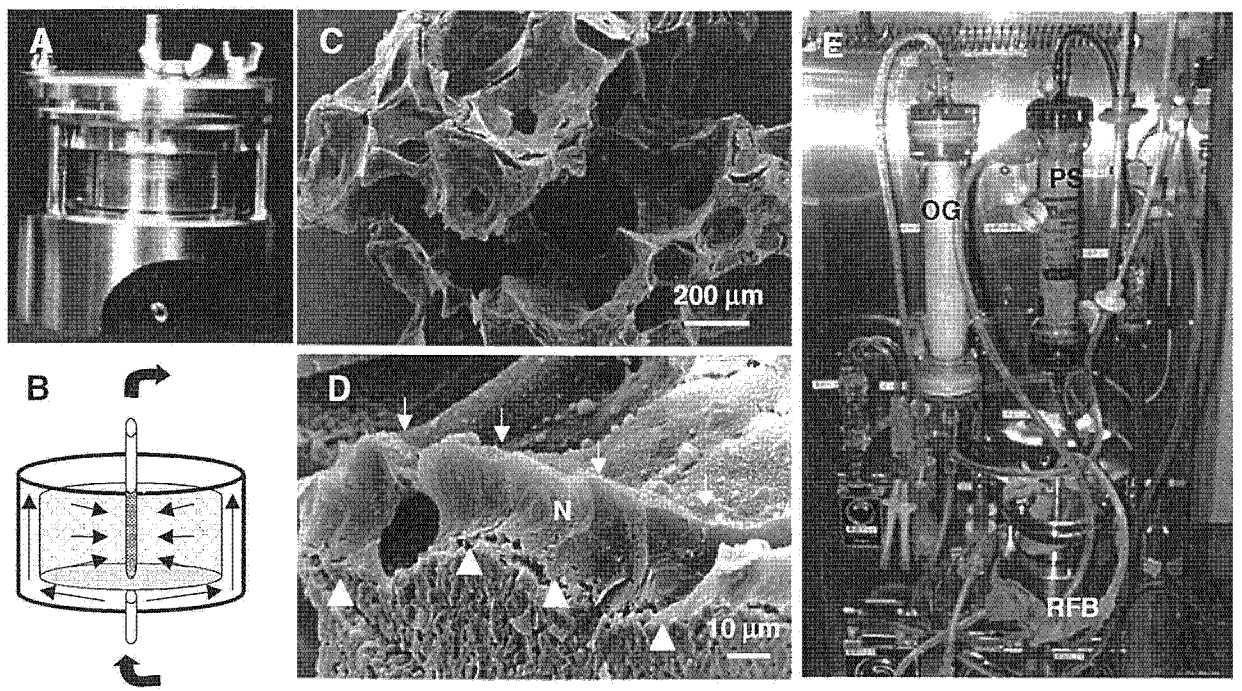

FIG. 1. (A,B) The RFB. The RFB is packed with cell-adhesion scaffolds in a cylindrical array. Culture medium or plasma flows from the periphery of the cylindrical module to the center. (C,D) Scanning electron microscopic (SEM) observations in FLC-4 cells cultured on hydroxyapatite beads in the RFB. FLC-4 cells form a single layer on porous hydroxyapatite beads in a cubic array. The arrow heads indicate the basal side of cells, while the arrows show the apical side of cells. N, nucleus. (E) The extracorporeal BAL system. From blood obtained from an artery, and plasma is separated from cells at 10–15 mL/min by the plasma separator (PS) and flows into the BAL after taking up oxygen from the oxygeneter (OG). The entire device is maintained consistently at 37°C. The purified plasma is mixed with blood cells and returned to a vein.

glucose solution and 7% sodium bicarbonate were injected as required during the monitoring of venous blood glucose and arterial blood acid-base parameters.

BAL using the RFB

The RFB (Biott, Tokyo, Japan) is a cell-filling type bioreactor of 15-mL capacity in which a cylindrical module is filled up with porous hydroxyapatite beads (PENTAX, Tokyo, Japan) with a diameter of approximately 1 mm (1) (Fig. 1A,B,C). The culture system consists of the RFB, a reservoir-adjusting culture fluid, a circulation pump, and an automatic controller to adjust the dissolved oxygen content and the pH of the culture fluid. We injected 10^8 of FLC-4 cells, a human HCC cell line, into the reservoir, which contained ASF 104 culture medium (Ajinomoto, Tokyo, Japan) with 2% fetal bovine serum (FBS) and set the circulated pump at 10 mL/min for seeding and attaching cells into the porous hydroxyapatite beads in the RFB (Fig. 1D). The circulation culture at 25 mL/min was continued for 10 days after adhesion of the cells was confirmed and FLC-4 cells grew 10^9 in the RFB. We used the RFB almost completely filled with cells as the BAL.

Extracorporeal circulation using the RFB

Arterial blood was extracted at 20–30 mL/min, and plasma was separated at 10–15 mL/min by a plasma separator (Plasmaflo, OP-02W, Asahi Kasei Medical, Tokyo, Japan) and allowed to circulate through the BAL after passage through an oxygenator (silicone rubber tube module M40-3000, Nagayanagi, Tokyo, Japan) (Fig. 1E). The entire device was maintained constantly at 37°C. Together with the separated blood cells, the purified plasma was returned to the animal via the cervical vein. The extracorporeal circulation time in this experiment was 4–6 h. Intravenous treatment with 50% glucose and 7% sodium bicarbonate solution continued after the BAL extracorporeal circulation. Heparin was injected as an anticoagulant. At initiation of extracorporeal circulation, an intra-

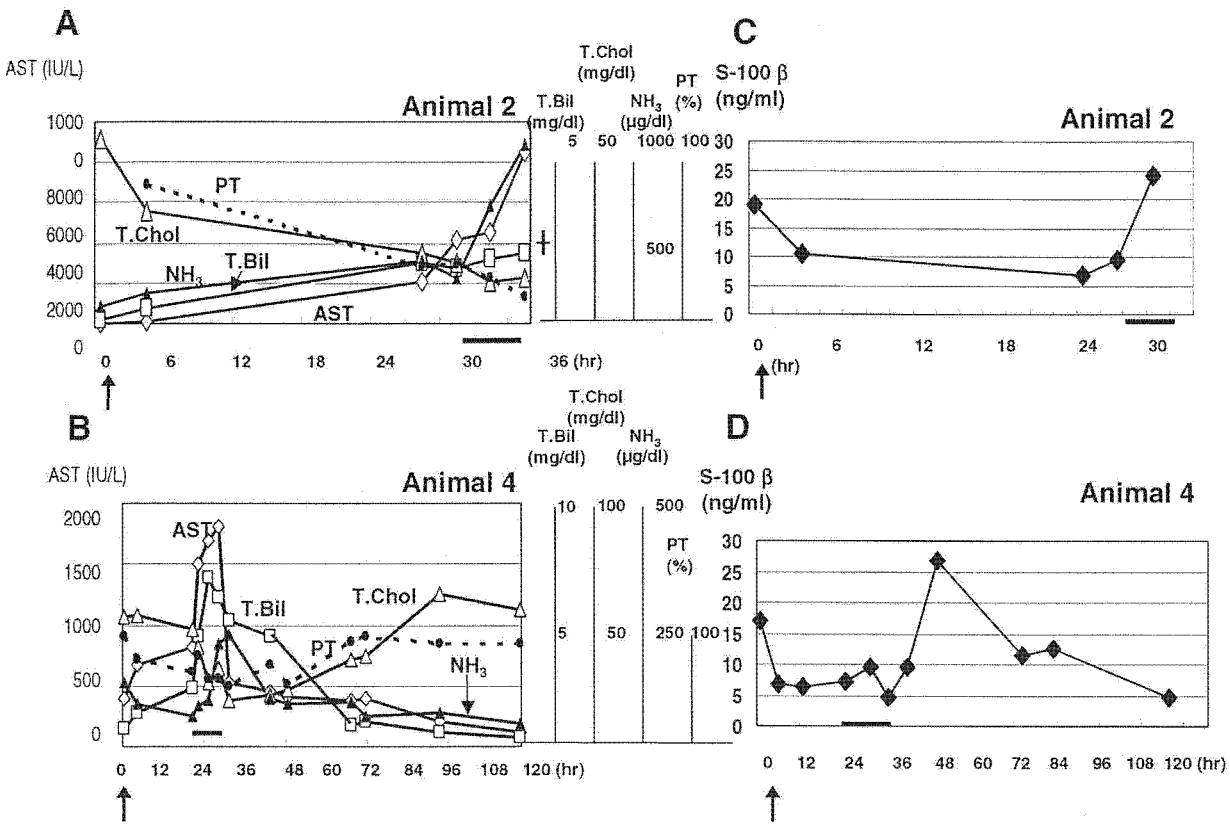

FIG. 2. (A) Time course of biochemical data in control (animal 2) developing hepatic failure after administration of α-amanitin and LPS. Plasma was perfused through the RFB without FLC-4 cells. Neither control animal (animals 1 and 2) recovered at any time from fatal hepatic failure. (B) Time course of biochemical data in an animal (animal 4) developing acute hepatic failure after administration of α-amanitin and LPS. Plasma was perfused through the RFB containing FLC-4 cells beginning 12 h or more after toxin administration. All three animals (animals 4, 5, and 6) treated by BAL therapy survived. The arrow indicates the time of α-amanitin and LPS administration. Black bar indicates extracorporeal BAL perfusion. AST, aspartate amino transferase; T.Bil, total bililbin; T.Chol, total cholesterol; PT, prothrombin time. (C) S-100 β protein in plasma from an animal with untreated acute hepatic failure, showing a marked increase that suggested severe astrocytic damage. (D) This increase is less prominent during BAL extracorporeal circulation.

venous injection of 1000 units was given. Heparin then was infused into the withdrawn arterial blood at 500 units/h.

Enzyme-linked immunosorbent assay (ELISA) for S-100 β in plasma

We measured S-100 β protein in plasma as a systemic marker of damage to brain astrocytes in pigs with acute hepatic failure using an ELISA kit (Yanaihara Institute, Shizuoka, Japan).

RESULTS AND DISCUSSION

In the present preclinical study, our ultimate aim was to find a way to prevent or reverse potentially lethal hepatic encephalopathy in acute hepatic failure using BAL as a bridge to either recovery or transplantation. We used an acute hepatic failure model involving a relatively large animal to test the effectiveness of densely cultured FLC-4 cells in a module for extracorporeal circulation. Devising an acute hepatic failure model in a relatively large animal is extremely difficult. We used the method of Takada et al., who induced acute hepatic failure by injecting α-amanitin and LPS via the portal vein (4). We first established extracorporeal circulation through a BAL system without FLC-4 cells in two animals (animals 1 and 2) with α-amanitin/LPS-induced hepatic dysfunction. The animals died respectively 2 h after initiation of extracorporeal circulation and at a completion point of extracorporeal circulation at 6 h (Fig. 2A). We thus used the BAL system with FLC-4 cells to treat hepatic dysfunction

in three animals (animals 3, 4, and 5), obtaining EEG improvement and survival in all. Figure 2B shows the course of one animal treated by BAL therapy. Even when transaminase and ammonia concentrations in blood were not markedly elevated, many animals that had been injected with α-amanitin and LPS died of hemorrhagic necrosis of the liver with marked cerebral edema. Among the blood tests, the best index of hepatic failure was a decrease in the cholesterol concentration. We therefore administered BAL for 4–6 h, when the EEG showed slowing and plasma cholesterol decreased, about 12–20 h after toxin administration. The three animals with acute hepatic failure showed considerable normalization of slow-wave activity in the EEG after extracorporeal circulation therapy using FLC-4 cultured in the RFB, with ultimate survival.

The reason for the survival of animals with acute hepatic failure treated with the BAL is thought to be the prevention of rapidly progressive cerebral edema. In plasma from a pig dying from hepatic failure, and a surviving animal just after BAL therapy, we measured the plasma levels of S-100 β protein as a marker of hepatic encephalopathy specifically astrocytic damage (3). S-100 β protein had significantly increased in plasma from animals with acute hepatic failure, especially those that died (Fig. 2C). In contrast, we observed that the release of S-100 β protein in plasma was inhibited during BAL therapy and the animal survived (Fig. 2D). This suggested that BAL therapy tended to ameliorate encephalopathy in acute hepatic failure.

Agents potentially responsible for hepatic coma include not only ammonia and manganese compounds, but also an assumed unknown substance with a molecular weight of 5–20 kD (5). Astrocytes form the blood brain barrier (BBB), and sustain nerve cells as they function (6). Increases of the postulated hepatic coma agent in blood induce early functional impairment in astrocytes. However, removal of the unidentified hepatic coma agent(s) is difficult using conventional blood-purifying treatments. We therefore feel an urgent need to develop modalities such as the BAL, in which human liver cells (highly functioning HCC cell lines) are cultured at high density in an RFB. The results of this experiment suggest that BAL can ameliorate hepatic encephalopathy by removal of suspected and/or unknown hepatic coma agents.

CONCLUSIONS

We constructed a compact and high functional BAL system using the RFB and a human HCC cell line FLC-4. Large animals with acute hepatic failure induced by α-amanitin and LPS were able to recover from fatal hepatic encephalopathy, and the result was improved by the extracorporeal circulation therapy using this system.

Acknowledgments: We thank Mr. H. Saito at the Jikei University School of Medicine for SEM technical support, and the technicians of the Division of Central Clinical Laboratory at Jikei University Hospital for blood and biochemical analysis. We also thank the 21 medical students of the Jikei University School of Medicine for their involvement in carrying this study as part of our practice-of-research program between 2001 and 2004.

This study was supported in part by Grants-in-Aids from the University Start-Ups Creation Support System, The Promotion and Mutual Aid Corporation for Private Schools of Japan, and The Japan Health Sciences Foundation (Research on Health Sciences for Drug Innovation, KH71068).

REFERENCES

1. Iwahori T, Matsuura T, Maehashi H, et al. Cyp3a4 inducible model for in vitro analysis of human drug metabolism using a bioartificial liver. *Hepatology* 2003;37:665–73.
2. Saito M, Matsuura T, Masaki T, et al. Reconstruction of liver organoid using a bioreactor. *World J Gastroenterol* 2006;12: 1881–8.
3. Hovsepyan MR, Haas MJ, Boyajyan AS, et al. Astrocytic and neuronal biochemical markers in the sera of subjects with diabetes mellitus. *Neurosci Lett* 2004;21:224–7.
4. Takada Y, Ishiguro S, Fukunaga K, et al. Increased intracranial pressure in a porcine model of fulminant hepatic failure using amatoxin and endotoxin. *J Hepatol* 2001;34:825–31.
5. Yamazaki Z, Fujimori Y, Sanjo K, et al. New artificial liver support system (plasma perfusion detoxification) for hepatic coma. 1978. *Ther Apher* 2000;4:23–5.
6. Matsushita M, Yamamoto T, Gemba H. The role of astrocytes in the development of hepatic encephalopathy. *Neurosci Res* 1999;34:271–80.